Regulation of Growth Factor Productions and related Biological Functions Using Anthocyanidin and Human Milk Oligosaccharides

June 2022

Annisa Krama

Regulation of Growth Factor Productions and related Biological Functions Using Anthocyanidin and Human Milk Oligosaccharides

A Dissertation Submitted to
the School of the Integrative and Global Majors,
the University of Tsukuba
in Partial Fulfillment of the Requirements
for the Degree of Doctor of Philosophy in Food Innovation
(Doctoral Program in Life Science Innovation)

Annisa Krama

Abstract

Growth factors are secreted as an active molecule which affect the growth of cells by stimulating a variety of cellular process including cell proliferation, migration, differentiation, and morphogenesis during development and tissue healing. The modulation of growth factors is important in term of their functions to maintain tissue homeostasis. Hepatocyte growth factor (HGF) and vascular endothelial growth factor (VEGF) are one of the growth factors which are considered as promising therapeutic agents. Some studies have been reported their advantages in promoting tissue regeneration. The abnormal productions of HGF and VEGF is crucial for cancer development. Cyanidin 3-glucoside (C3G) and human milk oligosaccharides (HMOs) which are food-derived components have been reported their beneficial effects for human health by modulating cellular mechanisms. However, the investigations of their roles in growth factor modulation are still limited. In current study, the author found that C3G (50 μM) promoted HGF production levels from Normal Human Dermal Fibroblast (NHDF) cells in dose- and time-dependent manners by upregulating transcription of *HGF* gene via PKA pathway. C3G increased the phosphorylation of cAMP-response element binding protein (CREB) through the elevation of intracellular cAMP levels, and stimulated transcriptional activity of cAMP response element (CRE) by targeting β_2 – adrenergic receptor (β_2AR). In addition, the author demonstrated that HMOs suppressed VEGF effects to stimulate angiogenesis-like morphology in HUVECs co-cultured with TNF-α-treated Caco-2 cells. In these investigations, HMOs were found to suppress HUVECs morphology which was evaluated in scratch assay and tube formation assay. Further investigations are required to confirm these effects, by investigating downstream's effects of C3G-stimulated HGF production and performing quantitative analysis to confirm HMOs' suppression effects on VEGF. This study demonstrated the potentials of C3G and HMOs to provide therapeutic and prevention effects in certain diseases by modulating growth factors.

Keywords: growth factor, food-derived components HGF, VEGF, C3G, HMOs.

Table of contents

Abbreviations

LDH	Lactate dehydrogenase
C3,5-diGlu	Cyanidin 3,5-diglucoside
C3G	Cyanidin 3-glucoside
cAMP	Cyclic adenosine monophosphate
CRE	cAMP rensponse element
EGF	Epidermal growth factor
FGF	Fibroblast growth factor
HEK293	Human embryonic kidney 293 cells
HGF	Hepatocyte growth factor
HMOs	Human milk oligossacharides
NHDF	Normal human dermal fibroblast
HUVECs	Human umbilical vein endothelial cells
Caco-2	Human colon carcinoma cell line-2
pCREB	Phosphorylated cAMP-response element-binding protein
PKA	Protein kinase A
TNF-α	Tumor necrosis factor alpha
VEGF	Vascular endothelial growth factor
β_2AR	Beta2-adrenergic receptors

Chapter 1

General introduction

1.1 Growth factors

A growth factor is defined as a biomolecule which affects the growth of cells by stimulating a variety of cellular process including cell proliferation, migration, differentiation, and morphogenesis during development and tissue healing[1]. Growth factors are capable to promote signal transduction by acting on specific cell surface receptors, leading to signal activation to other intracellular components, then eventually result in altered gene expression[2]. Many growth factors are peptides (2-50 amino acid residues) or proteins (more than 50 amino acid residues) which typically bind with high affinity to a specific plasma-membrane-bound protein. The binding site of these growth factors in their receptors is on the outer cell membrane surface (extracellular domain). In addition, cytokines, comprising small peptides, are also considered as growth factors if they are able to promote cell growth or differentiation signaling pathway. For examples, granulocyte-macrophage colony-stimulating factor (GM-CSF) was found as a growth factor because it promotes the production of white blood cells by stem cells[3]. Some lipid-soluble steroid hormones, including estrogen, androgen, and progestogens, also act as a growth factor which is produced by glands and secreted into the circulatory system. These steroid hormones directly pass through the cell's plasma membrane, bind to an intracellular protein receptor, and then transmit a growth signal[1, 4].

1.2 Food-derived components

1.2.1 Natural products

Natural products are any pharmacologically or biologically active chemical substances in nature commonly extracted from the plants and other living organisms such as phenolic compounds, dietary fibers, polysaccharides, vitamins, carotenoids, pigments, and oils. They are relatively small molecules with a molecular weight below 3,000 Daltons and present in structural diversity. They can provide beneficial effects and have various kinds of biological activities, particularly when they are

consumed as food or dietary supplements[5]. Furthermore, they can be potentially isolated from a metabolically engineered organisms by which the chemical structure has been determined and the resultant compound is chemically equivalent to the native natural products[6, 7] Natural products also have similar term as secondary metabolites that are not essential for the growth and development, but generally act in the survival of the organism which acts as a defense mechanism[8].

Flavonoids are the most abundant polyphenols produced as secondary metabolism products of plants including chalcones, flavones, flavonols, isoflavonols, and anthocyanin. Over 4000 types of flavonoids have been discovered in food and beverages of plant origin, including glycosides and acylglycosides that are commonly found in fruits and vegetables. Dietary flavonoids such as flavonols and flavones are majorly found in onions and teas, respectively[9]. In higher plants, as belong to a class of low-molecular-weight phenolic compounds, flavonoids are produced in particular site of the plants and beneficial to promote growth and development of seedlings, defense against plaque by acting as UV filter, and protect plants from biotic and abiotic stresses. Their occurrence is usually recognized as flower pigments in angiosperm families but is also found in all parts of the plants[10].

1.2.2 Anthocyanin and cyanidin 3-glucoside (C3G)

Anthocyanins are highly water-soluble pigment, predominantly occurred in the outer cell layers, responsible to give colors in plants, flowers, and many fruits such as cranberries, black currants, red grapes, merlot grapes, raspberries, strawberries, blueberries, and blackberries. Based on its basic structure, anthocyanin is kind of glycoside consisted of two or three parts of aglycon base (termed anthocyanidin), sugars, and possibly acylating groups. To obtain an anthocyanin, the anthocyanidin must be combined with at least one sugar molecule, then anthocyanins are classified by the number of sugar molecules in their structures, such as glucose, galactose, rhamnose, and

arabinose. The anthocyanidin has two aromatic rings (A and B-rings/chromane ring) linked via C-C bonds through C-ring containing oxygen heterocyclic ring (Fig 1-1)[11, 12].

More than 90% of all variety of anthocyanins isolated in nature consist of 6 kinds of anthocyanidins based on six aglycones differing in their B-ring substitution pattern, namely cyanidin (cyd) about 50%, delphinidin (Dp), pelargodin (Pg) and peonidin (Pn) about 12% respectively, petunidin (ptd) and malvidin (mvd) about 7% respectively. However, most of anthocyanidin variety that is found in food resources is in the form of cyanidin. Furthermore, these aglycones are classified by the number of bonded sugars and the presence of aliphatic or aromatic carboxylates attached to their sugar moieties, including cyanidin 3-glucosides, 3-biosides, 3,5- and 3,7-diglucosides[13, 14].

Cyanidin 3- glucoside (C3G) is a glycoside within the anthocyanidin group that is abundant in mulberry and red fruit. The molecular formula of C3G is $C_{21}H_{21}O_{11}^{+}$, and its molar mass is 449.3843 g/mol[15]. C3G is also known as chrysanthemin and consists of an *O*-glycosylated anthocyanidin with two hydroxyls on the third aromatic ring. In addition, C3G presents in the carbinol form through flavylium cation hydration or in the quinoidal form through proton loss. Fig 1-2 shows the structure of C3G[14].

1.2.3 Human milk oligosaccharides (HMOs) as food macronutrients

Food macronutrients are classified as food-derived components comprising of carbohydrates, fats, and proteins. These components provide energy and possess unique structures required in human tissue. Human milk which is the perfect food for infants consists of 87% water, 7% carbohydrates, 4% fats, and 1% protein as food macronutrients. Among 7% carbohydrates, oligosaccharides in human milk are presented as 5-15 g/L, as the third largest solid component in human milk after protein and fat[16] .

Human milk oligosaccharides (HMOs) are non-digestible and structurally diverse complex carbohydrates. In this case, HMOs do not function to directly provide energy sources for the infants, but they are mostly utilized by specific infant gut bacteria. They are essential for selectively supporting the growth of specific bacteria, particularly bifidobacterial[17].

HMOs are structurally diverse unconjugated glycan, composed of both neutral and anionic species with building blocks of five monosaccharides: D-glucose (Glc), D-galactose (Gal), *N*-Acetyl-Glucosamine (GlcNAc), L-fucose (Fuc), and sialic acid (Neu5Ac) which are conjugated via several linkage types, such as via glycosidic bonds (Fig 1-3). Common HMOs (Table 1) contains disaccharide lactose core at their terminal position via the linkage of β1-4 glycosidic between galactose and glucose (Gal (β1-4) Glc) which is catalyzed by the lactose synthase protein complex[18].

HMOs are classified into 3 major structures consisted of fucosylated neutral HMOs such as 2'-fucosyllactose (2'-FL), accounted as 35-50% of total HMOs present in human milk; sialylated acidic HMOs such as 3'-sialyllactose (3'-SL) and 6'-sialyllactose (6'-SL) present in 12-14%; and non-fucosyllactose neutral HMOs present in 42-55% such as Lacto-N-neotetraose (LNnT) (Fig 1-4).

1.3 Previous studies on food-derived components in growth factors modulation

Several food-derived components show their therapeutic effects in modulating growth factors, thus provide multiple beneficial effects. Natural products have been investigated to modulate deleterious effects of pathological epithelial-to-mesenchymal transition (EMT) through different signal transduction pathways by targeting TGF-β1. Arctigenin (ARC) has been investigated to repress EMT by inhibiting phosphorylation and transcriptional activity of Smad2/3 induced by TGF-β1, and blocking snail and N-cadherin expression[19]. By showing these mechanisms, ARC has been proposed as an anti-inflammatory and anti-cancer agent. Betanin also showed potent

anti-oxidative and anti-inflammation activity by modulating specific markers of EMT such as TGF-β1, type IV collagen, α-SMA and E-cadherin expression. By regulating TGF-β pathway, betanin suppressed renal fibrosis in diabetic nephropathy[20]. Isoviolanthin also showed its inhibition effects of TGF-β-induced EMT by targeting TGF-β/Smad and PI3K/Akt/mTOR pathway in HepG2 and Bel-7402 HCC cells[21].

Recent articles showed piperonylic acid which is a natural small compound isolated from black (*Piper nigrum L.*) and long (*Piper longum L.*) pepper revealed epiodermal growth factor (EGF)-like activity by activating phosphorylation of ERK and AKT, and downstream gene expression via epidermal growth factor receptor (EGFR) activation. Furthermore, piperonylic acid promoted PLCγ1 and STAT3 activation, then consequently promoted keratinocyte growth and survival in human keratinocyte cells line (HaCat cells)[22].

In addition, another natural product elicited the inhibition effects of non-small cell lung cancer (NSCLC) growth. In NSCLC, about 30% patients carry the mutated EGFR. Overexpression of EGFR mutation activates downstream pathways such as PI3K/AKT and MPAK/ERK signaling causing tumor cell motility, adhesion, metastasis, and angiogenesis. Parthenolide which is found in *Tanacetum parthenium* has been discovered to exert anti-cancer activity by strongly binding to EGFR, thereby reducing phosphorylation of EGFR as well as its downstream signaling pathways. These mechanisms resulted in promoting growth inhibition and apoptosis in the NSCLC cells harboring EGFR mutant[23].

Resveratrol (RSV) is a natural phenolic compound isolated from plants, such as grapes and blueberries. RSV has been investigated its potential as antiangiogenic factor that affect fibroblast growth factor 2/fibroblast growth factor receptor (FGF2/FGFR) signaling pathway. In arthritic cartilage, overproduction of matrix-degrading enzymes by chondrocytes stimulates matrix degeneration. Furthermore, FGF-2 and IL-2 play roles as catabolic mediators to upregulate the

enzymes. One study showed that RSV inhibits the activations of catabolic mediators such as FGF-2 in the ERK/MAPK pathway resulting in suppressing effects of catabolic process involved in cartilage degeneration. Thereby, RSV was suggested to be potential as therapeutic compound for articular cartilage regeneration[24].

1.4 Motivation of research study

Growth factors are vital molecules to promote cellular proliferation, migration, differentiation, and morphogenesis during development and tissue healing. In normal condition, growth factors have remarkable effects on the wound healing process, for example EGFR, HGF, and VEGF, through stimulating proliferation and migration in early phase. However, the abnormal production and regulation of these growth factors can trigger disease progression, like cancers. Therefore, the modulation of growth factors is crucial to maintain their functions in normal behaviors.

Several studies on the regulation of growth factors through downstream signaling have been already reported. Furthermore, another mechanism to regulate growth factors is to modulate their production in upstream signaling pathway. This mechanism controls or modulates more effectively various downstream signaling regulated by growth factor, itself, rather than regulating only specific downstream pathway. EGFR triggers downstream signaling axes in two mechanisms by PI3K/Akt and MAPK signaling which in turn stimulates transcription factors, such as Myc, c-Fos, CREB, and NF-κB to activate target genes related with proliferation, angiogenesis, invasion, and metastasis[25]. Another example is vascular endothelial growth factor (VEGF) which is the most studied growth factor in angiogenesis activates downstream pathways including PI3K-Akt/mTORC2, Raf-MEK-MAPK, and Src-FAK pathways which promotes vascular permeability, cell proliferation, and cell motility in angiogenesis process[26]. A crosstalk between angiogenesis and inflammation state

involves pro-inflammatory cytokines (TNF-α, IL-1 IL-1α, IL1β) and NF-κB signaling pathway which is occurred in upstream signaling to activate VEGF-related pathways[27]. If the EGFR or VEGF production is modulated through upstream pathway, many cellular behaviors regulated by different pathways can be also modulated effectively. This advantage provides broad mechanisms of actions to study about cellular behaviors regulated in different pathways.

Nowadays, consumers shift to consume food products with enhanced health benefits to prevent degenerative diseases. To fulfill customer's needs, the development of new food products derived from natural products or food nutrients has been conducted a lot. Therefore, robust investigations related to biological processes describing beneficial effects of food-derived components is required to provide scientific evidence. Furthermore, food-derived components can be consumed as common diet to prevent several diseases by potentially affecting numerous growth factors, hormones, and molecules. Although previous studies focused on the regulation of growth factor functions by food-derived components, the studies about production of growth factors are still limited. Based on this motivation, this study focuses on the modulation effects of HGF and VEGF by food-derived components through upstream signaling pathway.

1.5 Hepatocyte growth factor (HGF): structures and biological functions

In 1984, HGF was firstly discovered as a mitogenic protein for rat hepatocytes showing regenerative effects in injured liver within only one week, so that HGF provided some roles in the regulation of liver growth and regeneration during injury. In the 70%-hepatectomized rats, HGF was discovered to be increased by distant organs such as lung, kidney, and spleen via endocrine manner for supporting liver regeneration via portal vein. Besides, HGF has been discovered to be enhanced via paracrine system. It was produced from neighboring cells such as Kupffer cells which was also required for morphological and functional recovery from hepatitis. The primary structure

of biologically active HGF was defined as a heterodimeric molecule which comprises 697 or 692 amino acids and consists of an α-chain and a β-chain. The α-chain contains four kringle domains and the β-chain contains a serine protease-like structure[28, 29].

HGF was similarly identified as scatter factor that was originally identified as a fibroblast-derived cell motility factor for epithelial cells[30]. HGF receptor was identified as *c*-Met proto-oncogene. The binding of active HGF to the *c*-Met receptor promotes the activation of *c*-Met tyrosine kinase and the autophosphorylation of tyrosine residues in *c*-Met leading to stimulation of various biological responses such as mitogenic, angiogenic, morphogenic, motogenic, and anti-apototic (Fig 1-5)[28, 29, 31].

In normal state, HGF- *c*-Met pathways play roles in modulating dynamic morphogenesis in tissue regeneration after injury, for example, tubulogenesis in renal tubular cells, and promoting cell survival in neuronal cells. In contrast, the activation of HGF- *c*-Met pathways in cancer tissue stimulates abnormal dynamic cell movement and survival supporting invasion-metastasis and resistance to anticancer drug[32]. Therefore, modulating HGF production is considerably essential in providing potential therapeutic effects through HGF- *c*-Met mediated pathways.

The applications of food-derived components in the modulation of HGF have been conducted. The extract of bitter melon pulp has been investigated to stimulate HGF production via MAPK pathway[33]. Other food-derived components such as daphnane diterpenoids from *Daphne odora* and caffeic acid derivatives have been also known as HGF inducers[34, 35]. However, the mechanisms of actions of these natural products to stimulate HGF production have not been investigated, yet.

1.6 Vascular endothelial growth factors (VEGF): biological functions in angiogenesis and inflammation state

VEGF-A is known as the most abundant VEGF produced by most cancer cells to promote tumor angiogenesis through the upregulation of hypoxia. *In vivo* study showed that VEGFR-2 is the main responder to VEGF-A in tumor angiogenesis. VEGF-A is a member of a family of VEGF-B, VEGF-C, VEGF-D, VEGF-E and placental growth factor (PIGF) proteins. VEGF-A is dominant variant in regulating angiogenesis and disease. VEGF receptor 1 (VEGF-R1) and VEGF-R2 predominantly bind to VEGF which exert as the main signaling receptor for VEGF. These receptors are also expressed on endothelial cells, take essential roles for endothelial cell differentiation (vasculogenesis) and for the sprouting of new capillaries from pre-existing vessels (angiogenesis) during development[36]. A specific interaction of VEGF with VEGFR-2 on the plasma membrane of endothelial cells results in the dimerization, kinase activation, and autophosphorylation of specific tyrosine residues within the dimeric complex for the activation of endothelial cells leading to the subsequent intercellular pathways. Consequently, this interaction is also required for proliferation, migration, survival, tube formation, cell-cell adherence junction, focal adhesion, and vascular permeability of endothelial cells to supply new blood vessels at the angiogenic diseases sites[37].

In addition, during inflammation process, cells damaged by infectious agents or cellular stress release endogenous molecules known as alarmins or danger-associated molecular patterns (DAMPs) that will be utilized by leukocytes to induce the activation of the inflammasome and NF-κB signaling pathway. This activation releases several pro-inflammatory cytokines such as VEGF, IL-1α, IL-1β, and TNF-α. Subsequently, these cytokines, particularly VEGF/VEGFR targets endothelial cells which then promote angiogenesis processes as downstream effects[38, 39].

A recent study showed that 3'-SL has potential effects as an anti-angiogenic agent by inhibiting the phosphorylation of VEGFR-2 by binding its VEGF binding site at the second and

third IgG-like domains, thus blocks downstream signal activation[37]. However, the potential effects of pooled HMOs in modulating VEGF-induced angiogenesis in the inflammation state have not been conducted well.

1.7 Purpose of study

The purpose of this PhD thesis is to investigate the potential bioactivities of food-related components on the modulation of HGF productions and VEGF's biological functions. In Chapter 2, the author focused on the investigations on the effects of C3G in HGF production levels in NHDF cells and its mechanisms of actions. In Chapter 3, the author investigated target estimation of C3G in promoting HGF production via PKA pathway. In Chapter 4, the author focused on the investigations on the effects of HMOs in suppressing VEGF-induced angiogenesis-like morphology in HUVECs cells co-culture with TNF-α-treated Caco-2 cells. The author expects this study contributes to highlight the potentials of food-derived components as preventive agent by modulating growth factors in the early stage of several diseases.

Table 1. Common HMOs and their chemical structure[18]

HMO	Abbreviation	Structure
2'-FL	2'-fucosyllactose	Fuc-α-(1→2)-Gal-β-(1→4)-Glc
3-FL	3-fucosyllactose	Gal-β-(1→4)-[Fuc-α-(1→3)]-Glc
LNT	lacto-*N*-tetraose	Gal-β-(1→3)-GlcNAc-β-(1→3)-Gal-β-(1→4)-Glc
LNnT	lacto-*N*-neotetraose	Gal-β-(1→4)-GlcNAc-β-(1→3)-Gal-β-(1→4)-Glc
LNFP I	lacto-*N*-fucopentaose I	Fuc-α-(1→2)-Gal-β-(1→3)-GlcNAc-β-(1→3)-Gal-β-(1→4)-Glc
LNFP II	lacto-*N*-fucopentaose II	Gal-β-(1→3)-[Fuc-α-(1→4)]-GlcNAc-β-(1→3)-Gal-β-(1→4)-Glc
LNFP III	lacto-*N*-fucopentaose III	Gal-β-(1→4)-[Fuc-α-(1→3)]-GlcNAc-β-(1→3)-Gal-β-(1→4)-Glc
LNDFH I	lacto-*N*-difucopentaose I	Fuc-α-(1→2)-Gal-β-(1→3)-[Fuc-α-(1→4)]-GlcNAc-β-(1→3)-Gal-β-(1→4)-Glc
LNDFH II	Lacto- *N*-difucohexaose II	Gal-β-(1→3)-[Fuc-α-(1→4)]-GlcNAc-β-(1→3)-Gal-β-(1→4)-[Fuc-α-(1→3)]-Glc
3'-SL	3'-sialyllactose	Neu5Ac-α-(2→3)-Gal-β-(1→4)-Glc
6'-SL	6'-sialyllactose	Neu5Ac-α-(2→6)-Gal-β-(1→4)-Glc
LST a	sialyl lacto-*N*-tetraose a	Neu5Ac-α-(2→3)-Gal-β-(1→3)-GlcNAc-β-(1→3)-Gal-β-(1→4)-Glc
LST b	sialyl lacto-*N*-tetraose b	Gal-β-(1→3)-[Neu5Ac-α-(2→6)]-GlcNAc-β-(1→3)-Gal-β-(1→4)-Glc
LST c	sialyl lacto-*N*-tetraose c	Neu5Ac-α-(2→6)-Gal-β-(1→4)-GlcNAc-β-(1→3)-Gal-β-(1→4)-Glc
DS-LNT	disialyl lacto-*N*-tetraose	Neu5Ac-α-(2→3)-Gal-β-(1→3)-[Neu5Ac-α-(2→6)]-GlcNAc-β-(1→3)-Gal-β- (1→4)-Glc
Type I chain		Gal-β-(1→3)-GlcNAc
Type II chain		Gal-β-(1→4)-GlcNAc

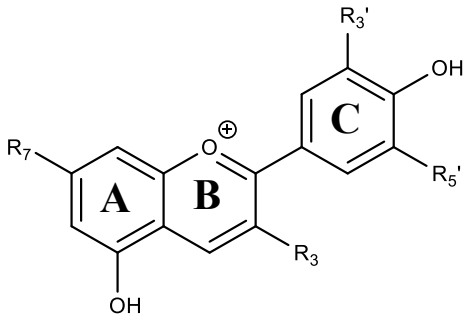

Figure 1-1. Basic structure of the most six types of anthocyanidin. Anthocyanidin has two aromatic rings (A and B-rings/chromane ring) linked via C-C bonds through C-ring. Pelargonidin (R_7, R_3 = OH), cyanidin (R_7, R_3, R_3'= OH), delphinidin (R_7, R_3', R_5'= OH), peonidin (R_7, R_3 = OH, R_3'= OCH_3), petunidin (R_7, R_3, R_3'= OH, R_5' = OCH_3), and malvidin (R_7, R_3 = OH; R_3', R_5' = OCH_3).

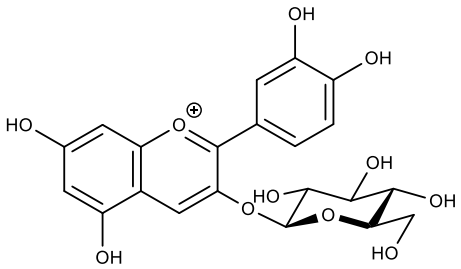

Figure 1-2. Chemical structure of cyanidin 3-glucoside

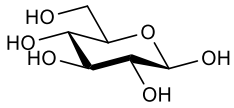

β-D-Glucose

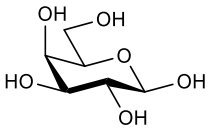

β-D-Galactose

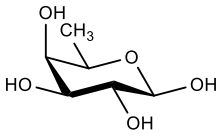

β-D-Fucose

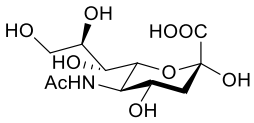

Sialic acid (N-Acetylneuraminic acid)

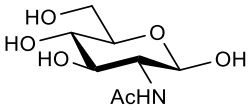

N-Acetylglucosamine

Figure 1-3. Structures of five monosaccharides in HMOs

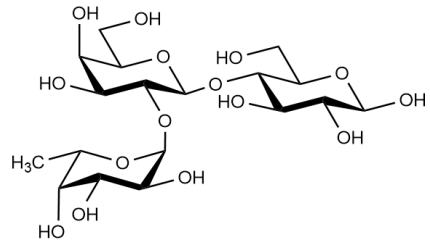

2’-fucosyllactose (2’-FL)

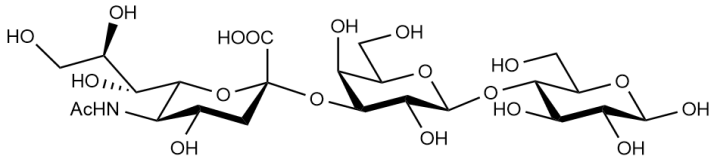

3’-sialyllactose (3’-SL)

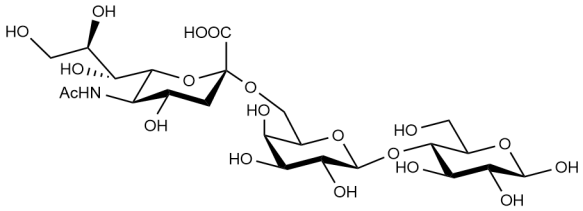

6’-sialyllactose (6’-SL)

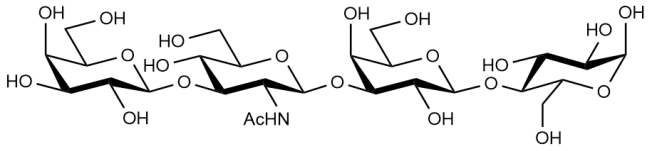

Lacto-*N*-tetraose (LNnT)

Figure 1-4. Chemical structures of individual HMOs

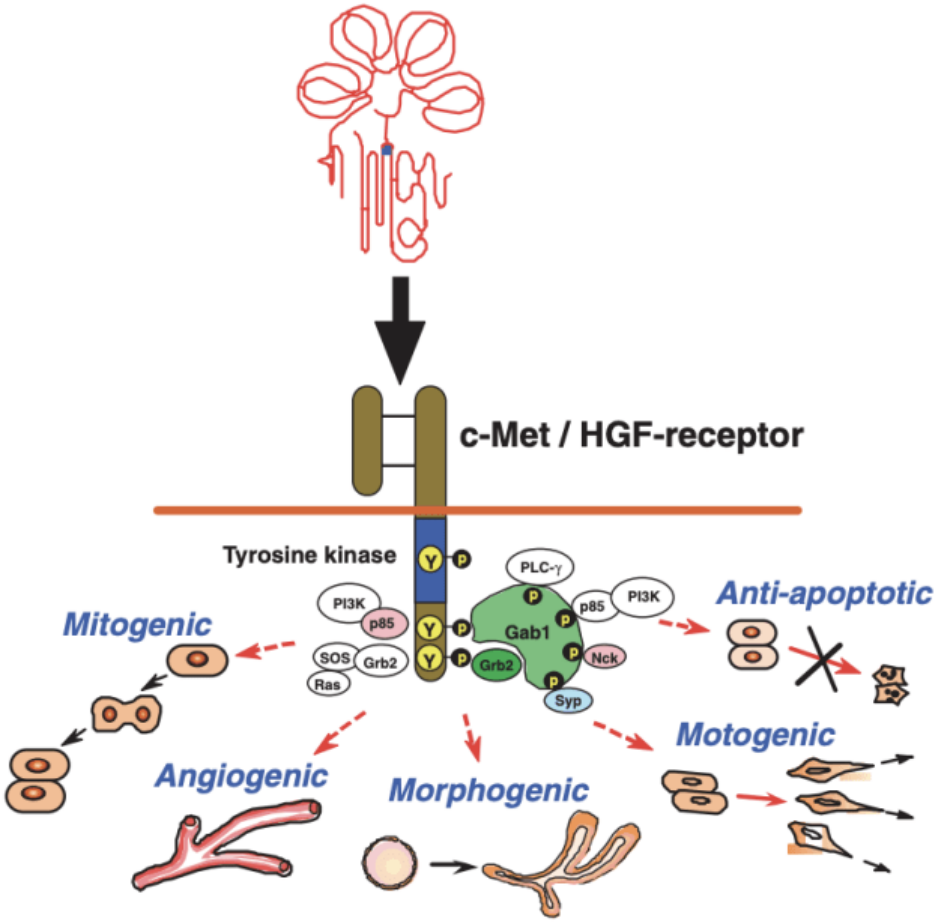

Figure 1-5. A variety of biological actions of HGF mediated via the c-Met (HGF-receptor). HGF receptor was identified as *c*-Met proto-oncogene. The binding of active HGF to the *c*-Met receptor promotes the activation of *c*-Met tyrosine kinase and the autophosphorylation of tyrosine residues in *c*-Met leading to stimulation of various biological responses such as mitogenic, angiogenic, morphogenic, motogenic, and anti-apototic. Adopted from *Physical and Biological Science*; **2010**, *86*, 588-610.

Chapter 2

Effects of C3G on the production of HGF in NHDF cells

2.1 Introduction

HGF is produced by stromal/mesenchymal cells as a single chain pro-HGF, which is cleaved into mature HGF at Arg^{494} and Val^{495} by HGF-activators such as urokinase-type plasminogen activator (uPA). HGF receptor is identified as *c*-Met protooncogene composing of structural domains that include the extracellular Sema, PSI, and IPT domains, the transmembrane domain, the intracellular juxtamembrane, and tyrosine kinase domains[28, 40]. HGF is considered as a candidate of therapeutic agent. In amyotrophic lateral sclerosis (ALS) mice model, the intrathecal administration of HGF attenuated motor neuron degeneration and prolonged the life span by 63% even after administration from the onset of paralysis[41]. In animal models for limb ischemia, intramuscular administration of either recombinant HGF protein or expression plasmid for HGF has facilitated new vessel formation, improved blood flow, and reduced muscle atrophy (potential for angiogenic growth factor)[42]. The most recent article showed that phase I/II study of intrathecal administration of recombinant human HGF (rhHGF) in severe model of cervical spinal cord injury showed significant functional improvements such as recovery of motor functional and axonal regeneration[43]. These studies showed that several approaches have been conducted to modulate HGF- *c*-Met pathways, such as development of recombinant HGF proteins, expression vector for HGF genes, and small-molecule HGF inducers[32].

Some natural products have been reported to show biological activities, by possibly modulating HGF production. In the previous study, screening assay was conducted with several natural products including tetrandrine, cyanidin 3-glucoside, acteoside, antimycin A3a, palmaerin A, palmaenone A, daphnodorin C, arctigenin, piceatamol, and scirpusin B. HGF production levels were measured by performing ELISA against conditioned medium collected from NHDF cells. C3G has been found to increase HGF production levels, much higher than other natural products (Fig. 2-1). According

to these results, the author focused on the investigations of potential effects of C3G in stimulating HGF production in NHDF cells.

C3G is the most abundant anthocyanin, which belongs to polyphenols, majorly found in plant-based foods. Such as leafy vegetables, berries, red cabbage, teas, and coloured grains. C3G has been known its potentials to provide antioxidant, anti-inflammation, and cytoprotective effects against various oxidative stress-induced disorders[14]. Recently, C3G has been discovered to improve several metabolic processes. One study reported that C3G improved skeletal muscle performance via oral administration to ICR mice by elevating the expression level of PGC-1α causing the increase of the expression level of mithocondrial biogenesis-related genes[44] : mitochondrial transcriptional factor A (TFAM) and mithocondrial genes (CPT-1β and UCP-3). This phenomenon could promote the increasing level of mitochondria in the skeletal muscle which is important to enhance exercise performance. Furthermore, C3G also plays important roles in promoting adipocyte by increasing C/EBP α expression and intracellular cAMP levels[44] and enhancing insulin sensitivity by increasing gene expression of C/EBP α, GLUT4 and insulin receptor protein expression[45]. However, the potential effects of C3G in promoting growth factor production in upstream signaling has not been conducted, yet.

In this chapter, the author aimed to investigate another scheme of beneficial effects of C3G as an inducer for HGF production in Normal Human Dermal Fibroblast (NHDF) cells. NHDF cells which derived from mesenchymal or stromal cells construct dermal layer in human skin was cultured in this study as an *in vitro* model to clarify the potential effects and mechanisms of action on HGF production in C3G treatment. NHDF was reported to secrete human HGF (hHGF), which was markedly enhanced by stimulation of several signaling pathways[46].

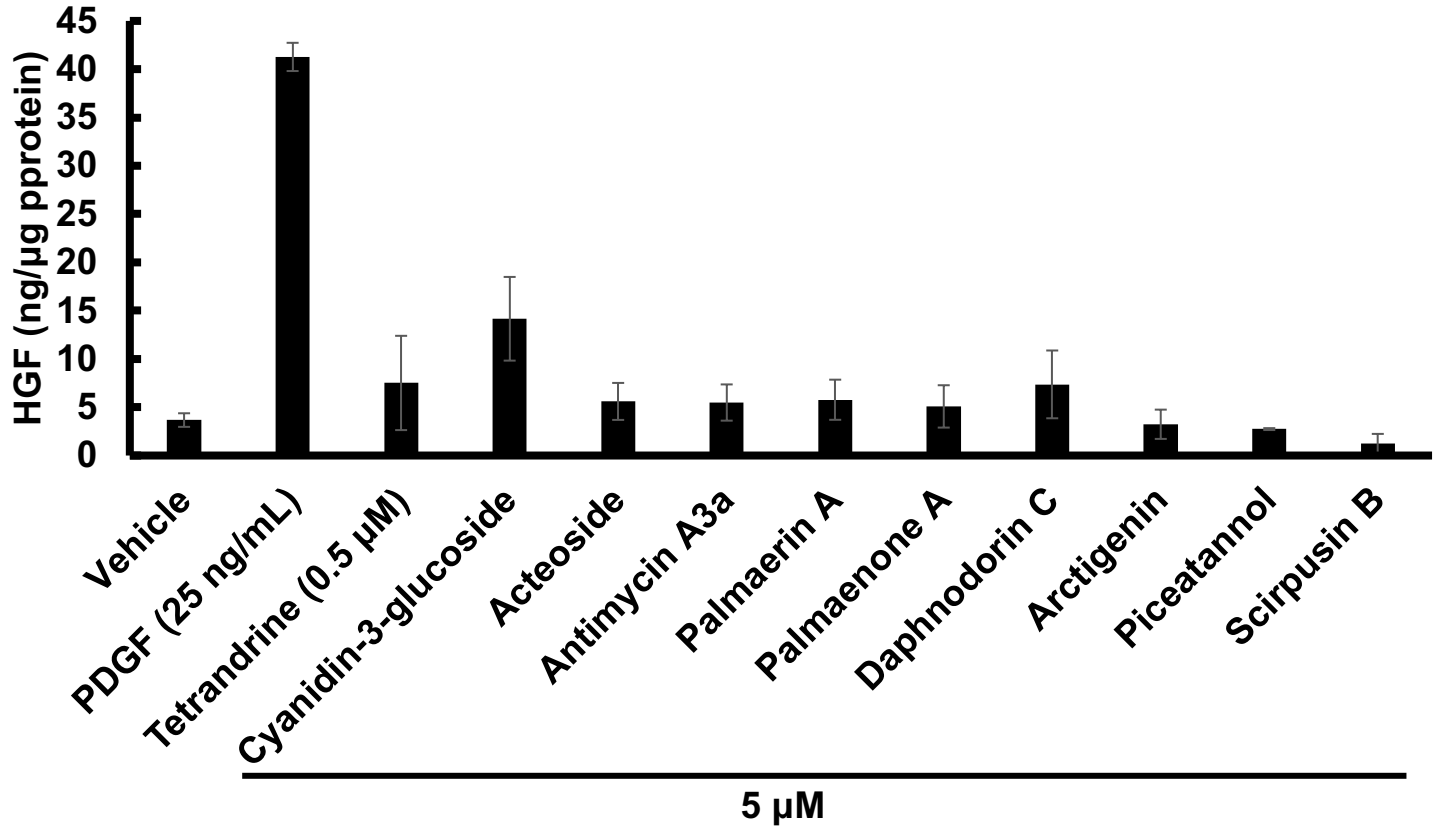

Figure 2-1. Screening assay of natural products in their potential effects to stimulate HGF production from NHDF cells. NHDF cells were seeded into 96-well plate until reaching 80% confluent. The next day, the cells were treated with vehicle (0.1% DMSO), PDGF-BB (25 ng/ml, shown as P), or active compounds at the indicated concentrations. Total HGF levels were quantified by using ELISA assay and calculated as final unit (ng/µg protein) after normalization with total protein concentrations. n = 5. This experiment was performed by Ms. Natsu Tokura.

2.2 Materials and methods

2.2.1. Test compounds

Test compounds used in this study were purchased from the following manufactures: Cyanidin 3-glucoside (Fuji Film Wako Pure Chemical Industries, Ltd, #633-42451NS380101), Cyanidin (Fuji Film Wako Pure Chemical Industries, Ltd, #030-21961), Cyanidin 3,5-diglucoside (Sigma-Aldrich, #74397), Platelet derived growth factor-BB (PDGF-BB) (Fuji Film Wako Pure Chemical Industries, Ltd, #166-19743), Forskolin (Nacalai, #16384-84), Isoproterenol (Nacalai, #19703-04), Rolipram (Tokyo Chemical Industry Co., Ltd, #D5835), 3-Isobutyl-1-methylxanthine (IBMX) (Fuji Film Wako Pure Chemical Industries, Ltd, #095-03413), KT5720 (Cayman Chemical, #10011011), H89 (Cayman Chemical, #10010556), PD98059 (ChemScene, #CS-0169), SP600125 (Cayman Chemical, #SP600125), SB203580 (Adipogen Life Sciences, #AG-CR1-0030), Bisindolymaleimide (Adipogen Life Sciences, #AG-CR1-0009), Wortmanin (Adipogen Life Sciences, #AG-CN2-0023).

2.2.2. Cell culture

The Normal Human Dermal Fibroblast (NHDF) cells purchased from Kurabo Co., Ltd, were cultured in Dulbecco's Modified Eagles Medium high glucose (DMEM) (SIGMA, #D5796) containing 10% fetal bovine serum (Gibco) at 37^{o}C in humidified 5% CO_2 incubator. After reaching 80% confluence, the NHDF cells were digested with 2 ml of 0.5g/l-trypsin in 0.53 mmol/l-EDTA solution (Nacalai Tesque, Inc, #32778-34), which subsequently were seeded into 96-well plate, 6-cm dish, and 6-well plate for ELISA, RT-PCR analysis, and western blotting analysis, respectively.

The Human Embryonic Kidney 293 cells (HEK293), provided from RIKEN Bioresource Research Center, were cultured in Dulbecco's Modified Eagles Medium high glucose (DMEM) (SIGMA) containing 10% fetal bovine serum (Gibco) and 1% of 100 U/mL Penicillin and 100

μg/mL Streptomycin (SIGMA, #11074440001) at 37ºC in humidified 5% CO_2 incubator. After reaching 80% confluence, the cells were seeded into 6-cm dish to be later transfected with recombinant plasmids for reporter assays.

2.2.3. Cell viability assay

3-(4,5-dimethylthiazol-2-yl)-2,5-diphenyltetrazolium bromide (MTT) assay (Dojindo, #M009) was performed to examine cell viability. Confluent NHDF cells were seeded into 96-well plate at a density of $1x10^4$ cells per well and the cells were incubated with the medium overnight. After incubation, the cells were treated with various concentrations of C3G (0.1, 1, 5, 10, 25, 50, or 100 μM) for 24, 48 or 120 h. Old medium was replaced to the fresh medium, then 10 μM MTT solution (5 mg/mL) was added to the cell culture overnight incubation until formazan crystals were observed. Subsequently, formazan crystals were dissolved in 100μL of 10% sodium lauryl sulfate (SLS) (Nacalai Tesque, Inc, #08933-05) and incubated overnight. After that, the absorbance was measured at 570 nm using microplate reader (Varioskan Lux).

2.2.4. HGF level quantification by enzyme-linked immunosorbent assay (ELISA)

Confluent NHDF cells were seeded into 96-well plate until reaching 80% confluent. The cells were treated with C3G at indicated treatment time. A day before ELISA experiment, the Nunc-immuno plate (Thermo Fisher Scientific, #167245) were prepared by adding 100 μL HGF monoclonal antibody (0.2 μg/ml) (R&D Systems, Inc, #294-HG-100/CF) to each well, then the plates were incubated overnight at 4ºC. On the next day, the monoclonal antibody solution was removed from the wells, followed by washing the wells with 200 μL of 1x TBS/T. 100 μL of blocking solution (1% BSA, 5% Tween 20, 5% sucrose were dissolved in PBS) was added into each well, and then the plates were incubated for 1 h at room temperature. After incubation, the

blocking solution was removed, and the plates were washed with 200 µL of TBS/T twice. Conditioned medium of treated cells was transferred to the subjected wells. HGF standards (0, 0.5, 5, 15, 30, and 50 ng/ml of HGF standard) (R&D Systems, Inc, #294-GMP-025) were also added to the different wells. The plates were incubated for 2 h at room temperature. After incubation, culture supernatant was removed from the wells and the wells were washed with 200 µL of TBS/T three times. Biotinylated goat anti-human HGF antibody (250 ng/ml, 100 µL) (R&D Systems, Inc, #BAF294) was added into each well and the plates were incubated for 1.5h at room temperature. The solution was removed, and the plates were washed with 200 µL of TBS/T three times. Streptavidin conjugated horseradish peroxide (HRP) 200 ng/ml, 100 µL) (SIGMA, #RABHRP3) was added, then the plates were incubated for 30 minutes at room temperature. The solution was removed, and the plates were washed with 200 µL of TBS/T three times. Mixture solution of 35% H_2O_2 (Nacalai Tesque #V2B1044) and 0.3 mg/ml of 2,2'-Azino-bis (3-ethylbenzothiazoline-6-sulfonic acid) diammonium salt (ABTS) (Sigma-Aldrich, #10102946001) at a ratio 1:1000, respectively, was added 100 µL into each well, then the plates were incubated for 30 minutes at room temperature. After that 50 µL stopping solution (H_2SO_4) were added into each well. Absorbance was measured at 410 nm. Total HGF levels were calculated as final unit (pg/µL) after normalization with total protein concentrations.

2.2.5. BCA assay

BCA assay (Takara, #T9300A) was performed to determine total protein levels in NHDF cells after treatment. Attached cells were washed with PBS twice, then 50 µL lysis buffer (50 µL Triton-X (SIGMA) in 10 mL PBS) was added into each well. The plates were shaken for 20-30 minutes to get cell lysate. 25 µL of cell lysate was transferred into another 96-well plate.

Subsequently, 200µL of mixture solution A and B (100:1) was added into each well. The plates were incubated for 30 minutes at 37ºC. Absorbance value was measured at 570 nm.

2.2.6. RNA extraction

RNA samples were isolated from the treated cells by using ISOGEN kit (Nippon Gene Co., Ltd, #311-02501). Initially, the cells were washed with PBS, followed by addition of 1 ml of ISOGEN reagent. The cell suspension was mixed well and added with chloroform (0.2 ml). After mixing with vortex for 15 seconds, the mixture was stored for 3 minutes at room temperature, then centrifuged (12,000 x g for 15 minutes, at 4ºC). Aqueous phase was collected and mixed with 0.5 ml of isopropanol. The solution was stored for 10 minutes at room temperature, and then centrifuged (12,000 x g for 15 minutes, at 4ºC) until precipitate was obtained. After removing supernatant, 1 ml of 70% ethanol was added to the precipitate. The solution was then centrifuged (7,500 x g for 5 minutes, at 4ºC). The resultant precipitate was dried after removing supernatant, then 50 µL of RNAse free water was added to the dried precipitate. Concentrations of total RNA samples were measured by NanoDrop™ (Thermo Scientific).

2.2.7. cDNA synthesis

RNA samples (500 ng/µL) were used to synthesize cDNA. Superscript VILO Master Mix (Invitrogen by Thermo Fisher Scientific, #11755050) was mixed with RNA samples and RNAse-free water to adjust the total solution of 20 µL. Thermal cycler (Thermal Fisher Scientific) was used to amplify cDNA synthesis by following conditions: annealing primers (25ºC for 10 minutes), reversing transcribe RNA (50 ºC for 10 minutes), and inactivating enzyme (85ºC for 5 minutes). Concentrations of total cDNA samples were measured by NanoDrop™ (Thermo Scientific).

2.2.8. mRNA HGF level quantification by RT-PCR analysis

cDNA samples (500 ng/µL) were used as a template. RT-PCR analysis was performed by 7500 FAST Real-Time PCR (Applied Biosystems) using Thunderbird™ SYBR qPCR Mix (Toyobo, #QPS-201T). Briefly, 1 µL of primer set was mixed with SYBR qPCR mix solution (10 µL). Primer sequences were follows: HGF forward primer (5'-ACGAACACAGCTTTTTGCCTT-3'), HGF reverse primer (5'-AACTCTCCCCATTGCAGGTC-3'), ACTB forward primer (5'-CTGTGGCATCCACGAAACTACC-3'), ACTB reverse primer (5'-GCAGTGATCTCCTTCTGCATCC-3'). The mixture was added into 0.04 µL ROX reference dye and cDNA samples (1 µL), then filled with DNAse/RNAse water to adjust the total solution of 20 µL. . The analysis was performed with specific conditions as follows: holding stage (50 °C, 20 second; 95°C, 1 minute); cycling stage (95 °C, 15 second; 60 °C, 1 minute, 40 cycles); melting curve stage (95 °C, 15 seconds; 60 °C, 1 minute; 95 °C, 30 second; 60 °C, 15 second). The levels of mRNA HGF were calculated as relative levels compared to ACTB.

2.2.9. Gel preparation

Running gel (10%) was prepared by mixing the following order: 3.33 ml Acrylamide 30(w/v)%-Acrylamide/Bis Mixed Solution(37.5:1) (Nacalai Tesque, Inc, #07175-75), 2.5 ml resolving buffer 1.5 M Tris-HCl pH 8.8, 4.2 ml ddH_2O, 100µL of 10% sodium lauryl sulfate (SLS) (Nacalai Tesque, Inc, #), 60µL of 10% ammonium persulphate solution, and 10 µL TEMED PlusOne solution (GE Healthcare Life Life Science). Stacking gel was prepared by mixing the following order: 1 ml Acrylamide 30(w/v)%-Acrylamide/Bis Mixed Solution(37.5:1) (Nacalai Tesque, Inc), 0.75 ml stacking buffer 1.5 M Tris-HCl pH 6.8, 4.25 ml ddH_2O, 60µL 10% sodium lauryl sulfate (SLS) (Nacalai Tesque, Inc, #08933-05), 30µL of 10% ammonium persulphate solution, and 7 µL TEMED PlusOne solution (GE Healthcare Life Life Science, #17-1312-01).

2.2.10. Western blotting analysis

Confluent NHDF cells were seeded to 6 well-plate and treated with test samples. The NHDF cells were washed with PBS twice, then lysed with radioimmunoprecipitation (RIPA) buffer (Nacalai Tesque, Inc, #16488-34) mixed with 1% phosphatase inhibitor cocktail (Nacalai Tesque, Inc, #07575-51). The cell lysate was sonicated with following conditions: 5 second, pulse 1.1, Amp1 20%. Subsequently, the lysate was centrifuged (13,000 rpm, 10 min, 4 ºC). Total protein concentration in cell lysates was determined by BCA assay. Equivalent protein aliquots were separated by 10% SDS-polyacrylamide gel electrophoresis (PAGE) and transferred to Immobilon-P PVDF membrane (Merck Millipore, #IPVH00010). Anti-phospho-CREB (Ser133) (87G3) rabbit monoclonal antibody (Cell Signaling Technology, #9198S) which was diluted in TBS/T at a ratio 1:1000, was used to probe the blots, followed by incubation at 4 ºC overnight. The membrane was washed by TBS/T solution, then incubated for 1 h at room temperature with anti-rabbit immunoglobulin (IgG), HRP-linked antibody (Cell Signaling Technology, #7074) which was diluted with TBS/T at a ratio 1:3000. The protein expressions were detected with immobilon western chemiluminescent HRP substrate (Merck Millipore) using LuminoGraphI (WSE-6100, ATTO Corporation, Japan). After detection of phosphor-CREB, the membrane was re-probed with anti-GAPDH antibody (ThermoFisher Scientific, #MA5-15738). The membrane was washed with MiliQ twice, then were shaken with 10 ml of WB stripping solution strong (Nacalai, #05364-55) for 3 h at room temperature. After that, the membrane was rinsed with TBS/T solution, and shaken with 5% of skim milk in dissolved in TBS/T as blocking solution, then incubated at 4 ºC overnight with anti-GAPDH antibody which was diluted with TBS/T at a ratio 1:3000. The membrane was washed by TBS/T, then incubated for 1 h at room temperature with anti-mouse IgG, HRP-linked antibody (Cell Signaling Technology) which was diluted in TBS/T at a ratio 1:3000. The protein expressions were detected using the same method as above.

2.2.11. Statistical analysis

Statistical analyses were performed using GraphPad Prism9. Methods and representative symbols are described in the legends of the figures. Symbols mean significant differences from mean values of indicated numbers of independent experiments. A paired Student's *t*-test or one-way ANOVA followed by Tukey's test were used to compare different variables between two or more experimental groups, respectively. For all analyses, *p*-values below 0.05 were considered statistically significant and were indicated in the legends of the figures.

2.3 Results

2.3.1. Effects of C3G treatments on NHDF cell viability

NHDF cells were treated with C3G in different concentrations (0.1, 1, 5, 10, 25, or 50 μM) for 24, 48, or 120 h treatment. Compared to vehicle groups, C3G-treated NHDF groups showed higher cell viability levels, suggesting that C3G did not have cytotoxicity effects on NHDF cells (Fig 2-2).

2.3.2. Effects of C3G treatments on HGF production levels from NHDF

To examine the effects of C3G on HGF production levels from NHDF, the cells were treated with C3G with different concentrations (1, 5, 20, or 50 μM) in various incubation time (24, 48, 72, 96, or 120 h), then HGF levels were quantified by ELISA. In this study, platelet derived growth factor-BB (PDGF-BB: 25 ng/ml) was used as a positive control for stimulation of HGF production. Previously, PDGF-BB was found as the major motogenic factor in human serum for human dermal fibroblast to stimulates migration upon cell attachment to a collagen matrix, which

was essential for skin wound healing[47]. As shown in Figure 2-3, C3G enhanced HGF production at each time treatment in a dose-dependent manner in which the maximum dose (50 μM) of C3G showed stimulation of HGF levels in time-dependent manner. These results clearly suggested that C3G had stimulation effect of HGF production in NHDF cells.

2.3.3. Effects of C3G treatments on the expression levels of mRNA HGF

The expression levels of *HGF* gene were investigated in the presence of C3G by performing a real time RT-PCR. Figure 2-4 showed that the treatment of C3G (50 μM) enhanced mRNA abundance of *HGF* gene almost twice compared to vehicle groups, indicating that C3G promoted upregulation of *HGF* gene transcription.

2.3.4. Effects of co-treatment of C3G and various pathway inhibitors on HGF production levels from NHDF cells.

Next, the author examined which pathway may be involved in the promoting effects of C3G on HGF secretion from NHDF cells. The cells were treated with different inhibitors of various pathways and the levels of HGF secretion in the presence of inhibitors were quantified by performing ELISA (Fig. 2-5). The results showed that only co-treatment of C3G (50 μM) and KT5720 (1 μM) could hinder the secretion of HGF from NHDF, indicating lower levels of secreted HGF compared to the C3G treatment alone. Another PKA pathway inhibitor known as H89 was also used. Hereinafter, to observe H89 inhibition effects of HGF stimulation by C3G, the author also performed H89 treatment alone and co-treatment of C3G (50 μM) and H89 (10 μM). As the author expected, H89 treatment alone was able to reduce HGF levels until 22% compared to the C3G treatment groups, then this inhibition effects were also occurred in the co-treatment groups by 20% decrease rate (Fig. 2-6). These results suggested that PKA inhibitors (KT5720 and H89)

prevented the promoting effects of C3G on HGF production, suggesting that C3G may act through PKA pathway to stimulate HGF production from NHDF cells.

2.3.5. Effects of C3G treatment on the level of phosphorylated CREB

PKA pathway involves the elevation of cAMP levels which then activate several signaling pathways with protein kinase that can phosphorylate cAMP-response element-binding protein (pCREB) at serine 133[48]. Here, the author analyzed the phosphorylation of CREB in NHDF cells exposed to C3G. Forskolin was used as the cAMP elevating agent because its ability to activate adenylate cyclase that catalyze cAMP activation in PKA pathway[49]. The western blotting analysis showed that forskolin (1 μM) strongly enhanced the expression of pCREB. In addition to forskolin, C3G (50 μM) also increased the expression of pCREB (Fig. 2-7).

2.4 Discussion

HGF has been known to be stimulated by several natural products. The extract bitter melon pulp enhanced HGF production through the activation of MAPK pathway[33]. Caffeic acid derivatives consist of phenylethanoids and phenylpropanoids, which bear cathecol moiety in their structure, act as HGF inducer in NHDF cells. Furthermore, Nakasone *et al.,* reported that daphnane diterpenes, known as PKC modulator, also enhanced HGF production in NHDF cells[35]. However, detailed mechanisms of these compounds have not been investigated yet. In this study, the author discovered that C3G stimulated HGF productions in NHDF cells at protein and mRNA levels in dose- and time- dependent manner without cytotoxicity at several concentrations.

In addition to natural products, some synthetic compounds also regulated HGF production through specific mechanisms of actions. Small molecule drug such as 12-*O*-tetradecanoylphorbol 13-acetate (TPA) stimulated HGF secretions from human endometrial stromal cells (ESC) through

Protein Kinase C (PKC)-dependent pathways[50]. Phorbol 12-myristate 13-acetate (PMA) also stimulated HGF secretion and expression in U87 astrocytoma through PKC-dependent pathways, by showing inhibition effects of HGF expression by a PKC inhibitor, Go6976, specific for PKCα and PKCβ1[51]. According to these studies, the author also examined which pathway that supported HGF production in the presence of C3G by conducting screening analysis of co-treatment between C3G and several pathway inhibitors. Figure 2-5 and 2-6 showed the promoting effects of C3G in HGF production were cancelled in the co-treatment of C3G and PKA inhibitors, such as KT5720 and H89. These inhibitors which exert non-specific PKA inhibitors, are derived from a fungus *Nocardiopsis* sp and from an isoquinoline derivative, respectively. They have been already known as potent inhibitors for cAMP- specific PKA pathways, through similar mechanisms as competitive antagonist of binding site of ATP on PKA catalytic subunits[52, 53]. These results demonstrated that C3G promoted HGF production in NHDF cells via PKA pathway. In PKA pathway, adenylate cyclase (AC) catalyzes the conversion of adenosine triphosphate (ATP) into intracellular cyclic adenosine 3',5'-cyclic monophosphate (cAMP), a second messenger, which binds to PKA regulatory subunits. This binding promotes conformational change, releases PKA catalytic subunits which become bound to ATP, and promotes CREB phosphorylation in serine and threonine residues to activate transcriptional activity on specific target genes[54].

The author also investigated downstream signaling event of PKA activation promoting phosphorylation of the transcription factors CREB which is crucial for allowing binding of CREB protein with its transcriptional co-activator, CREB-binding protein (CBP) and p300, when bound to cAMP-response element (CREs) in target genes[55, 56]. In western blotting, the author found that the protein level expression of phosphorylated CREB (pCREB) was highly increased in the presence of C3G (50 μM) after 15 min treatment and reduced to the basal levels after 1 h treatment. Previous reports also showed the rapid increased of pCREB in the presence of forskolin and

PDGF-BB after 15 min treatment[57, 58]. This result suggested that C3G enhanced pCREB activation, which then led to promote *HGF* gene transcription. In conclusion, the stimulation effects of C3G on HGF production in NHDF cells were mainly regulated via PKA pathway.

In this study, the discovery of HGF stimulation effect by C3G may support further investigations on biological activities of HGF in downstream signaling, for example skin wound healing. Until now, there is no information about the roles of C3G-induced HGF in promoting skin wound healing in fibroblast and keratinocytes, particularly via PKA pathway. Therefore, in the future, the author is intrigued to investigate the biological effects of HGF stimulated by C3G in wound treatment involved in co-culture between fibroblast and keratinocytes, which highlights the implementation of C3G as a natural product in modulating HGF as therapeutic agent.

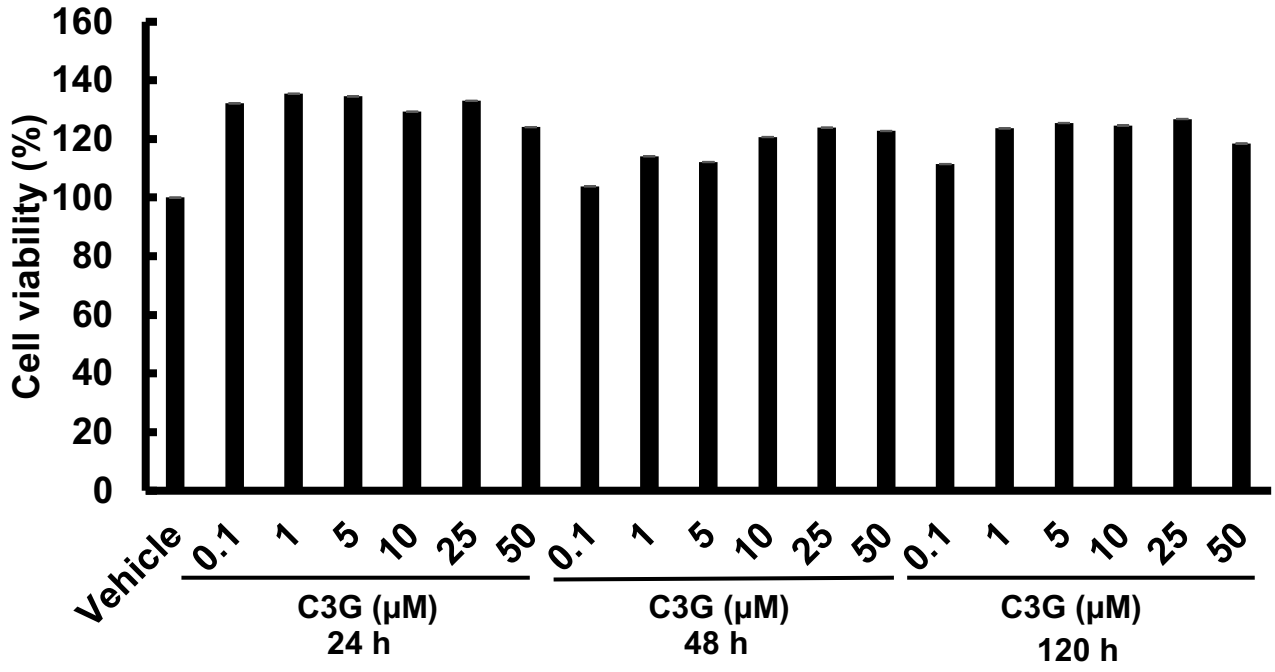

Figure 2-2. Effect of C3G on the cell viability of NHDF. NHDF cells were seeded into 96-well plate at a density of $1x10^4$ cells per well and the cells were incubated with the medium overnight. After incubation, the cells were treated with vehicle (0.1% DMSO, shown as -) or C3G at the indicated concentrations and monitored over time. The cell viability was measured using a MTT assay. n = 5.

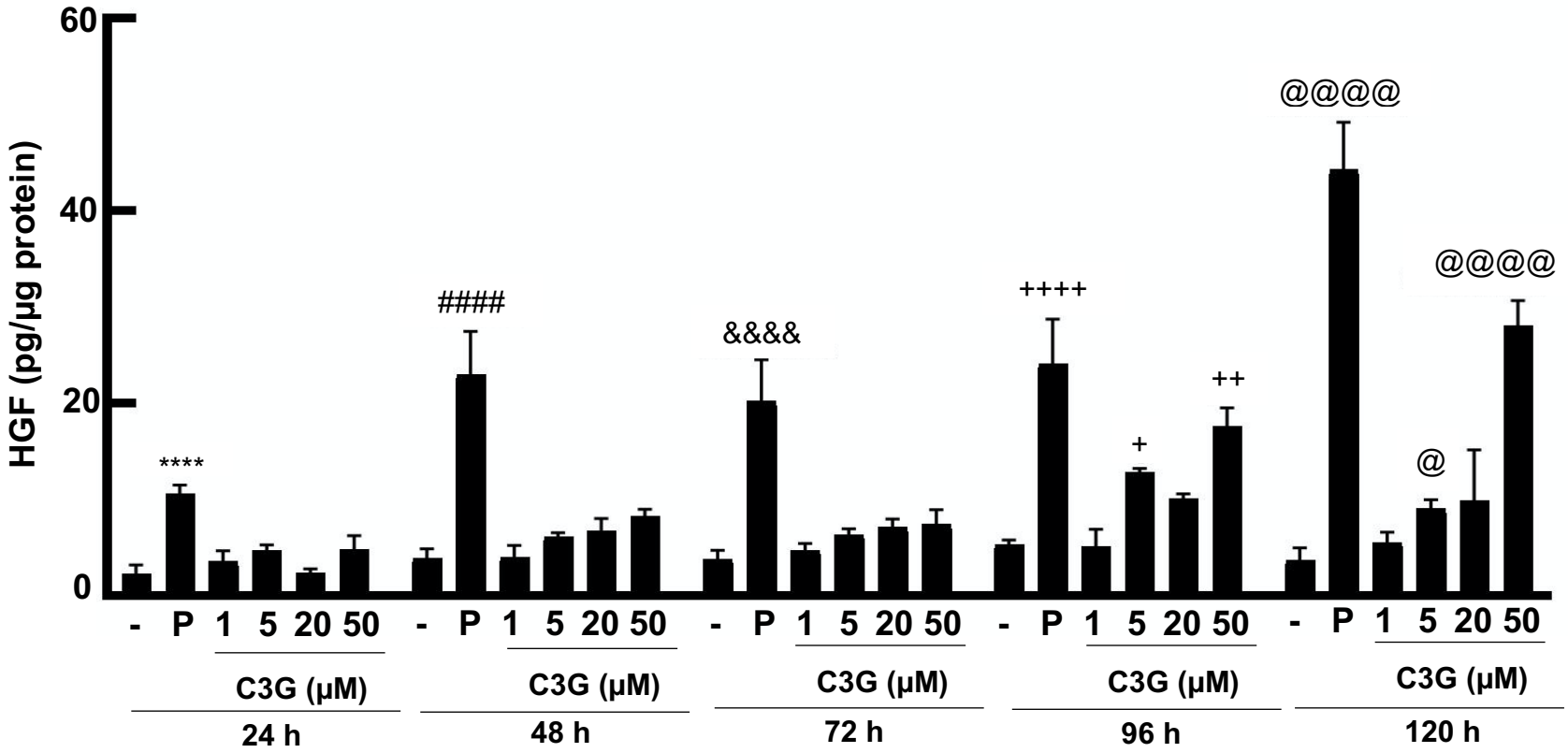

Figure 2-3. Effect of C3G on HGF production in NHDF cells. NHDF cells were seeded into 96-well plate until reaching 80% confluent. The next day, the cells were treated with vehicle (0.1% DMSO, shown as -), PDGF-BB (25 ng/ml, shown as P), or C3G at the indicated concentrations and monitored over time. Total HGF levels were quantified by using ELISA assay and calculated as final unit (pg/µg protein) after normalization with total protein concentrations. Statistical analysis was conducted using one-way ANOVA analysis (Tukey's test). Significant differences ($p < 0.0001$) versus vehicle at 24 h (****), 48 h (####), 72 h (&&&&), 96 h (++++), 120 h (@@@@). Significance difference ($p < 0.01$) versus vehicle at 96 h (++). Significant differences ($p < 0.05$) versus vehicle at 96 h (+) and 120 h (@). n = 5.

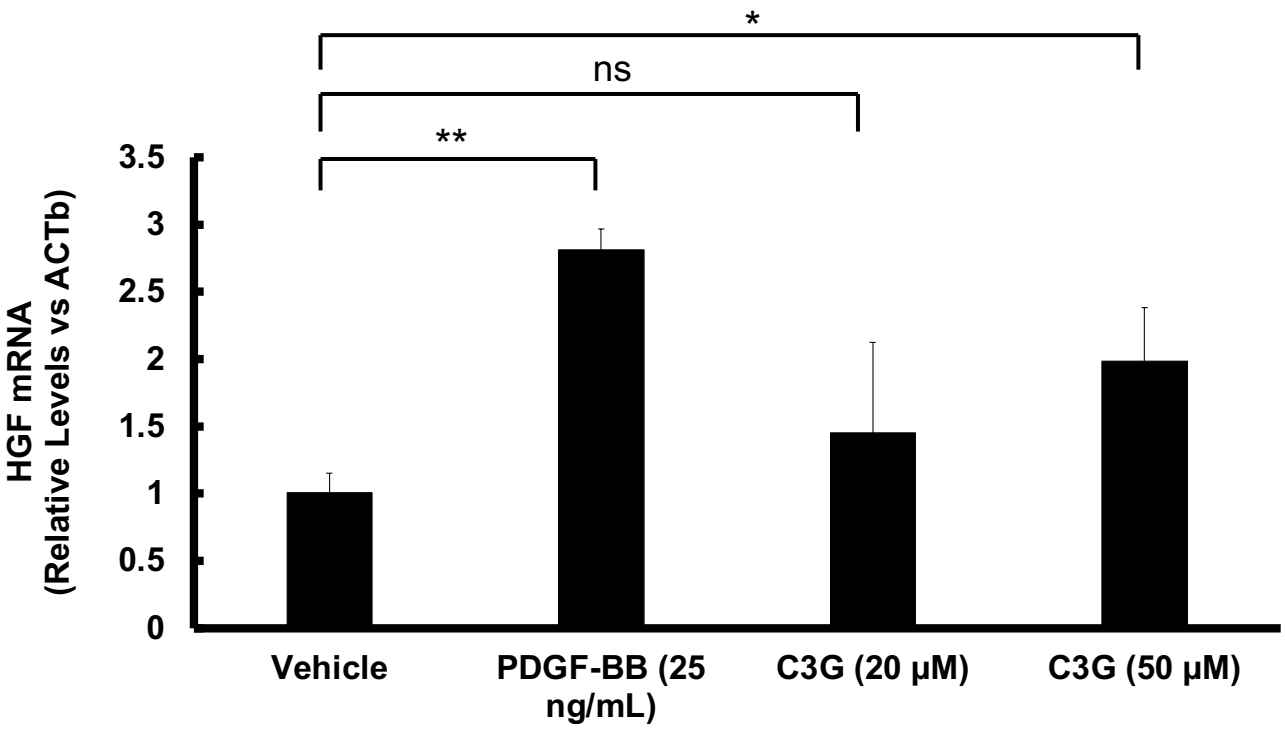

Figure 2-4. Effects of C3G on mRNA expression levels of *HGF*. Ninety percent confluent NHDF cells were seeded into 6-well plate and incubated overnight. The cells were treated with vehicle (0.1% DMSO). PDGF-BB (25 ng/ml), or C3G (20 or 50 µM) for 48 h. After that, RNA extraction and cDNA synthesis for RT-PCR analysis was performed. The mRNA levels of *HGF* were calculated as relative levels compared to *β-actin*. Statistical analysis was conducted using Student's *t*-test analysis. Significant difference (**$p < 0.01$, *$p < 0.05$) versus vehicle. $n = 3$.

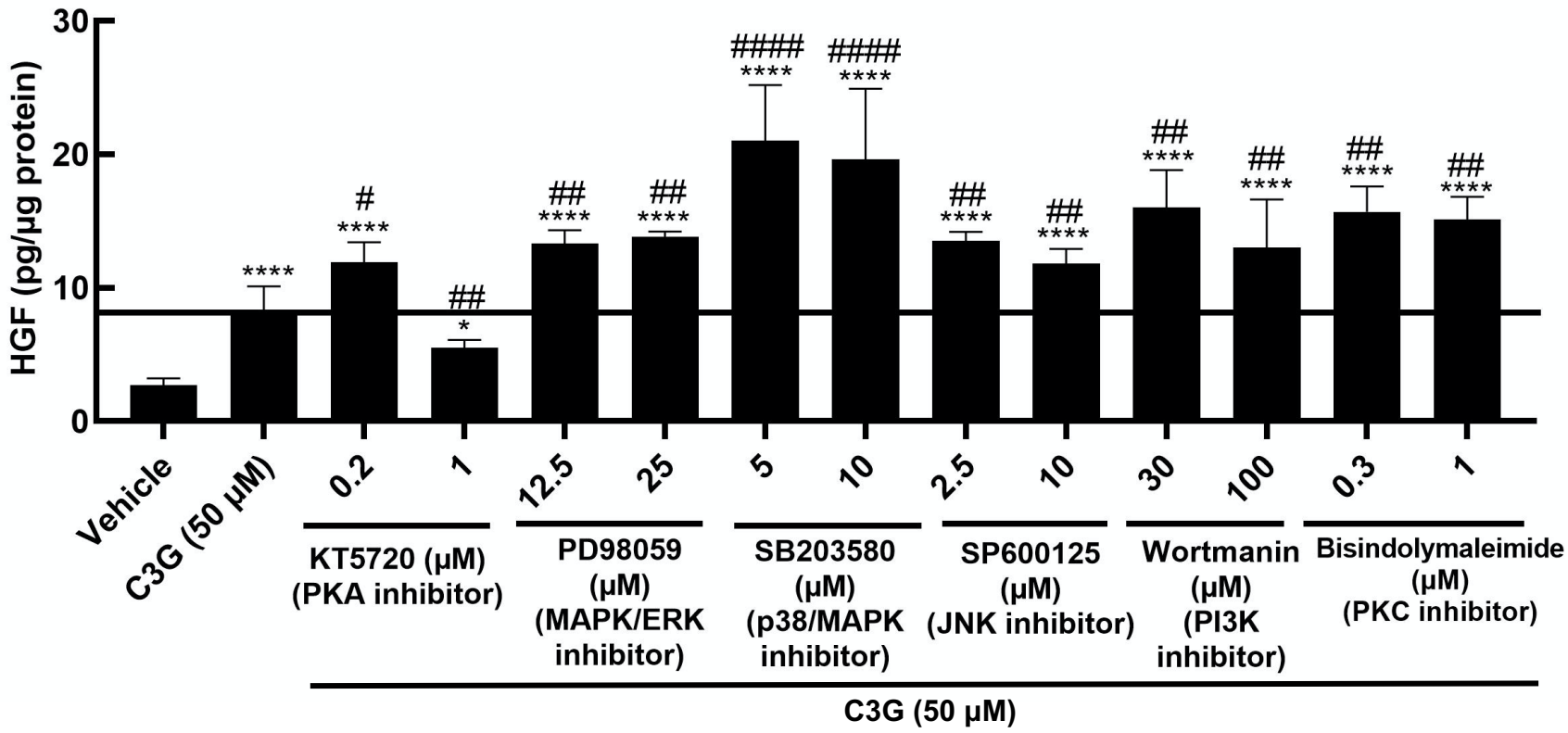

Figure 2-5. Effect of co-treatment of C3G and various pathway inhibitors on HGF production from NHDF cells. NHDF cells were seeded into 96-well plate until reaching 80% confluent. The cells were treated with vehicle (0.1% DMSO), and co-treated with C3G (50 µM) and pathway inhibitors at the indicated concentrations for 120 h. Total HGF levels were quantified by ELISA assay and calculated as final unit (pg/µg protein) after normalization with total protein concentrations. Statistical analysis was conducted using one way ANOVA analysis (Tukey's test). Significant difference (****p<0.0001, *p<0.05) versus vehicle. Significant difference (#### p<0.0001, ## p<0.01, # p<0.05) versus C3G 50 µM. n = 5.

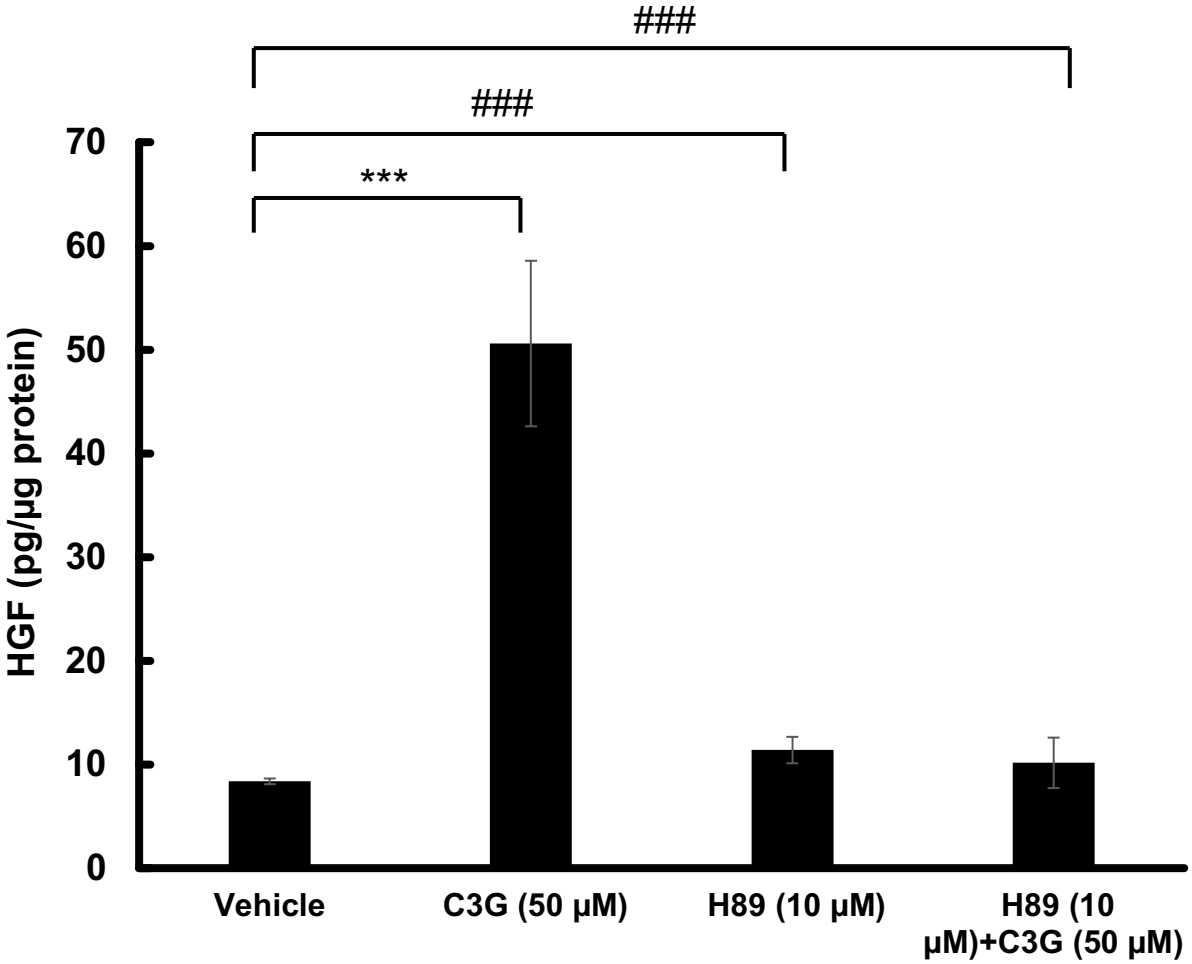

Figure 2-6. Effect of co-treatment of C3G and PKA pathway inhibitor on HGF production levels from NHDF cells. NHDF cells were seeded into 96-well plate until reaching 80% confluent. The cells were co-treated with C3G (50 µM) and H89 (10 µM) for 120 h. Total HGF levels were quantified by ELISA assay and calculated as final unit (pg/µg protein) after normalization with total protein concentrations. Statistical analysis was conducted using one-way ANOVA analysis (Tukey's test). Significant differences ($p < 0.01$) versus vehicle (***) or C3G treatment group (###). $n = 5$.

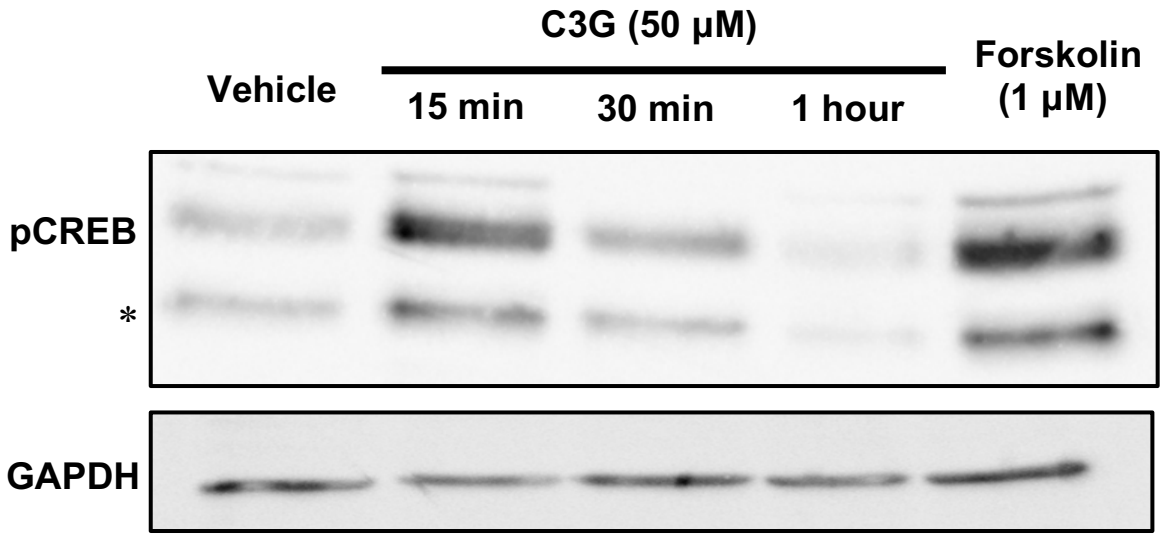

Figure 2-7. Effect of C3G on phosphorylation of CREB. NHDF cells were treated with C3G (50 μM) for 15 minutes, 30 minutes, or 60 minutes, and forskolin (1 μM) for 15 minutes. DMSO (0.1%) was used for vehicle group treatment. Cell lysates were immunoblotted with antibody against p-CREB. GAPDH is used for loading control. The phosphorylated form of ATF-1 at Ser63 is indicated as asterisk (*).

Chapter 3

Estimation of molecular target of C3G

3.1 Introduction

Natural products and their derivatives have become a vital source for new drug development since they consist of large number of substances with a range of biological activities. Polyphenols are one of examples for natural product which have attracted great interest in the field of medicine, food, and cosmetics because they have versatile functions as antioxidant, anti-cancer, and anti-bacterial. Polyphenolic structure such as catechol in natural polyphenols takes major responsibility for strong noncovalent interactions via multiple hydrogen bonding and hydrophobic interactions, and π–π interactions[59, 60].

Target identification of bioactive natural products becomes essential to elucidate their pharmacological activities through determination of mechanisms of actions which correlate with desired therapeutic effect for the prevention and treatment of a specific disease[61]. C3G has been reported as a master regulator of energy metabolism by directly acting as agonist of PPARs and exhibiting highest affinity for the PPARα demonstrating its efficacy to improve glucose tolerance and heaptic steatosis[62]. In the Chapter 2, the author has been elucidated the detailed mechanisms of C3G as a HGF inducer via PKA pathway showing a novel therapeutic function of C3G. Furthermore, exploring specific molecular target of C3G also supports further investigations on biological functions of HGF-induced C3G treatment.

G protein-coupled receptors (GPCRs) is a cellular surface membrane protein which responds to extracellular stimuli such as hormone and neurotransmitter leading to activate cellular signals by coupling to G proteins (G_s). GPCR is a well-known initiator of multiple signaling events which represents a major class of drug target, where more than 30% of the drugs approved by FDA are belong to this family[63]. β – adrenergic receptors (βARs) including β_1 -adrenergic receptor (β_1AR) and β_2 -adrenergic receptor (β_2AR) are belong to GPCRs with largest structures obtained so that providing many ligand recognitions and activation mechanisms[64, 65]. Upon binding to their

ligands, both β_1AR and β_2AR activation are also implicated to the activation of cAMP specific-PKA pathway[66]. Recently, Tripathi, *et al.* reported that quercetin as one of the flavonoids showed high affinity binding to β_2AR resulting a stimulation of cAMP production which led to increased alveolar fluid clearance via PKA pathway[67] suggesting that β_2AR activation had an biological effect for downstream signaling of PKA pathway. C3G is also a flavonoid which the structure is nearly similar with quercetin, so that the author assumed that C3G may be potential to interact with β_2AR. Furthermore, the investigation of β_2AR activation as a target for HGF production remains unclear. This background motivated the author to investigate β_2AR as a molecular target of C3G in promoting HGF via PKA pathway.

In addition, natural products-derived drug substances have multiple targets of proteins with multiple biological effects as well. The multitargeted interaction mode results in complexity which is required an accurate approach to identify the true targets of natural products[61]. In this case, introducing of foreign nucleic acids into cells is used to study the effects of expression of target genes, in short-or long-term. In this chapter, the author aimed to estimate molecular target of C3G in stimulating HGF production by using HEK293 cells which exogenously expressing β_2AR, then measuring the levels of CRE promoter activity and intracellular cAMP as indicators for PKA activation. The author found that these levels were increased only in β_2AR-dependent response indicating that C3G acted as an agonist for β_2AR, then the binding site of C3G was also estimated by comparing with other β_2AR ligands.

3.2 Materials and methods

3.2.1. Test compounds

Test compounds used in this study were purchased from the following manufactures: Cyanidin 3-glucoside (Fuji Film Wako Pure Chemical Industries, Ltd, #633-42451NS380101), Cyanidin (Fuji Film Wako Pure Chemical Industries, Ltd, #030-21961), Cyanidin 3,5-diglucoside (Sigma-Aldrich, #74397), Forskolin (Nacalai, #16384-84), Isoproterenol (Nacalai, #19703-04).

3.2.2. Cell culture

The Human Embryonic Kidney 293 cells (HEK293) provided from RIKEN Bioresource Research Center, were cultured in Dulbecco's Modified Eagles Medium high glucose (DMEM) (SIGMA) containing 10% fetal bovine serum (Gibco) and 1% of 100 U/mL Penicillin and 100 µg/mL Streptomycin (SIGMA, #11074440001) at 37ºC in humidified 5% CO_2 incubator. After reaching 80% confluence, the cells were seeded into 6-cm dish to be later transfected with recombinant plasmids for reporter assays.

3.2.3. Preparation of pcDNA3.1 vector and β_2AR DNA fragment

pcDNA3.1, with HA tag and recombinant β_2AR were amplified by following a protocol of KOD One PCR master mix (Toyobo, #KMM-101). Initially, mixture containing 12.5 µL KOD One PCR master, 10.5µL ddH_2O, 0.75 µL forward primer (5'-AAGCTTGCCACCATGTATCCGTATGATGTTCCGGATTATGCAGGGCAACCCGGGAAC-3'), 0.75 µL reverse primer (5'-CCCCTCTAGACTCGAGTTACAGCAGTGAGTC-3'), and 1 µL of 50 ng/ µL of template pcDNA3.1 vector (mNeonGreen-DEVD-NanoLuc, plasmid#98287) were subjected to thermal cycler (ThermoFisher), followed by addition of DpnI (Takara, #1235A) into 25 µL of PCR product, then incubated at 37ºC for 1 h, continuing to 80ºC for 15 minutes using heat block dry bath. After incubation, the DNA fragments of PCR products were separated by

performing gel electrophoresis and purified by following the protocol of Gel/PCR Extraction Kit (FastGene, Nippon Genetics, #FG91202). Vector map is shown in Figure 3-1.

3.2.4. Amplification of pGL4.29 and pGloSensor-22F cAMP plasmids

Reporter plasmids (pGL4.29) containing CRE-Luc reporter gene and pGloSensor-22F cAMP plasmids were purchased from Promega. The plasmid was transformed into a competent *Escherichia coli* (strain DH5-α). A single colony was inoculated in Luria-Bertani (LB) broth medium containing ampicillin and amplified. The plasmid was purified by following the standard protocol of FastGene plasmid mini kit (Nippon Genetics, #FG90402).

3.2.5. SLiCE reaction

DNA fragment encoding β_2AR was cloned into a pcDNA3.1 vector by performing SLiCE reaction[68]. Initially, pcDNA3.1 vector and β_2AR insert which were determined at ratio 1:1, were mixed with 1 µL of slice reagent and 1 µL of 10 x SLiCE buffer, then the mixture solutions were incubated at 37°C for 15 minutes using heat block dry bath. Finally, the recombinant β2AR plasmids were expressed and transformed in a competent *E.coli* (strain DH5-α). A single colony was inoculated in Luria-Bertani (LB) broth medium containing ampicillin, then it was isolated and purified by following the standard protocol of FastGene plasmid mini kit.

3.2.6. Transfection of HEK293 cells with pGL4.29 and treatment

HEK293 cells were seeded into 6-cm dish at a density of $1x10^6$ cells per dish and transfected with 4 µg of pGL4.29 plasmids by using Hily Max (Dojindo, #34291103). The transfected cells were incubated for 4 h at 37°C, then the medium was replaced with fresh medium. After that, the cells were incubated overnight at 37°C. The transfected cells were seeded into 24-

well plate and incubated overnight. The transfected cells were treated with test samples for 6 h incubations.

3.2.7. Co-transfection of HEK293 cells with pGL4.29 and pCDNA3.1- β_2AR plasmids

HEK293 cells were seeded into 6-cm dish ($1x10^6$ cells per dish), then the cultured cells were incubated overnight at 37°C in humidified 5% CO_2 incubator. The next day, the cells were co-transfected with pGL4.29 (4 µg) and pcDNA3.1- β_2AR (4 µg), or transfected with pGL4.29 (4 µg) by using Hily Max. The transfected cells were incubated for 4 h at 37°C, then the medium was replaced with fresh medium. After that, the cells were incubated overnight at 37°C. The transfected cells were seeded into 96-well plate and incubated overnight, and then treated with test samples for 24 h.

3.2.8. Cell lysate preparation and luciferase assay

The transfected cells treated with test samples were washed with PBS (-), then lysed with 100 µL of 1 x passive lysis buffer (Promega #V2B1044). Subsequently, the cells were shaken for 15 minutes to obtain cell lysate. After that, luminescence was measured by using Luciferase Assay Systems (Promega, #E1500) according to the standard protocol. Luminescence values (RLU) were quantified using microplate reader (Varioskan Lux, ThermoFisher).

3.2.9. GloSensor cAMP Assay

HEK293 cells were seeded into 6-cm dish ($1x10^6$ cells per dish), then incubated overnight at 37°C in humidified 5% CO_2 incubator. The cells were transfected with pGloSensor-22F cAMP (4 µg) and pcDNA3.1-β_2AR (4 µg) by using Hily Max. The transfected cells were incubated for 4 h at 37°C, then the medium was replaced with fresh medium. After that, the cells were incubated

overnight at 37ºC. The transfected cells were seeded into 96-well plate and incubated overnight. Then, transfected cells were equilibrated with equilibration medium containing GloSensor cAMP reagent (Promega, #E1290), and incubated for 2 h in room temperature. After that, pre-read kinetic measurement was conducted prior to test compound. Test compounds were added directly to the wells and kinetic assay of cAMP levels was measured by micro plate reader (Varioskan Lux).

3.2.10. ELISA assay

ELISA assay was performed by using the same method as previous chapter.

3.2.11. Statistical analysis

Statistical analyses were performed using GraphPad Prism9. Methods and representative symbols are described in the legends of the figures. Symbols mean significant differences from mean values of indicated numbers of independent experiments. A paired Student's *t*-test or one-way ANOVA followed by Tukey's test were used to compare different variables between two or more experimental groups, respectively. For all analyses, *p*-values below 0.05 were considered statistically significant and were indicated in the legends of the figures.

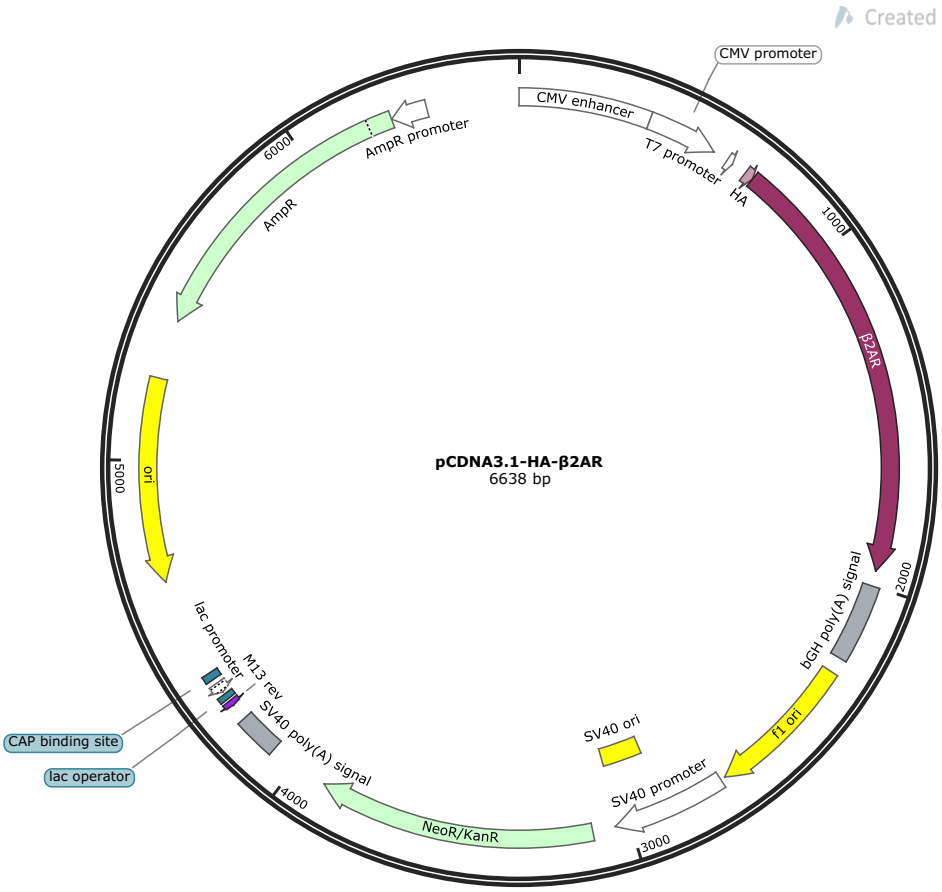

Figure 3-1. Vector Map of pcDNA3.1-HA-β_2AR.

The map was drawn by using SnapGene.

3.3 Results

3.3.1. Effect of C3G on promoter activity of CRE

In previous chapter, the author found that the mechanism of C3G on HGF production correlated with induction of phosphorylation of CREB, which was triggered by activation and translocation of PKA subunits. Phosphorylated CREB binds to a target sequence namely cAMP response element (CRE) which is also known as cAMP modulator to regulate target genes. In this study, the author used HEK293 cells transfected with pGL4.29 that contains CRE-Luc reporter gene in order to investigate the promoter activity of CRE-Luc in the presence of C3G alone and co-treatment of forskolin (5 μM) and C3G in different concentrations (12.5, 25 and 50 μM). The treatment of forskolin alone for 6 h enhanced the promoter activity 36 folds higher, compared to the vehicle groups. These levels were higher about 60 folds and 50 folds in the co-treatment of forskolin and C3G (25 μM) and co-treatment of forskolin and C3G (25 μM), respectively, compared to the forskolin alone (Fig. 3-2). This suggested that C3G and forskolin target distinct molecule for activation of CRE.

3.3.2. Effect of C3G on promoter activity of CRE in HEK293 cells expressing β_2AR

Next, to clarify specific target of C3G in stimulating HGF production via PKA pathway, the author focused on β_2AR, as one of the GPCR family receptors located in cellular surface membrane. Previous report showed β_2AR is expressed throughout the lung, alveolar air spaces, pulmonary lymphatics and vasculature and plays vital role in alveolar fluid balance[69]. β_2AR agonist such as salbutamol has been reported to improve the fluid balance in hypoxia condition. Recently, quercetin as flavonoid showed similar activity with salbutamol by showing higher binding affinity with β_2AR[67]. The author assumed C3G as another flavonoid may possibly to bind with β_2AR. To investigate whether C3G targets β_2AR, the author prepared HEK293 cells

transfected with pGL4.29 and the plasmid encoding β_2AR, then measured the promoter activity levels of CRE by luciferase assay. Treatment of C3G in β_2AR-expressed cells showed higher levels of CRE transcriptional activity in dose-dependent manner, while it did not induce the promoter activity in the cells transfected with only pGL4.29 (Fig. 3-3). These results suggested that C3G stimulated promoter activity of CRE via targeting β_2AR.

3.3.3. Effects of C3G on intracellular cAMP levels in HEK293 cells expressing β_2AR

To confirm that C3G may also act to enhance intracellular cAMP levels through the activation of β_2AR, the author prepared the cells transfected with pGloSensor-22F cAMP and the plasmid encoding β_2AR plasmid, then measured the intracellular levels of cAMP. The cAMP level was not affected by C3G in the cells transfected with pGloSensor-22F cAMP only (Fig. 3-4). however, the exogenous expression of β_2AR dramatically increased cAMP production at around 330 seconds after treatment (Fig. 3-4). These effects were also shown in dose-dependent manner (Fig. 3-5), suggesting that C3G enhanced cAMP levels via targeting β2AR.

3.3.4 Structure-activity study

To obtain more information about possible interaction between C3G and β_2AR, structure-activity studies on CRE-promoter activity and HGF production were assessed by using chemical derivatives of C3G such as cyanidin and cyanidin 3,5-diglucoside (C3,5-diGlc) (Fig. 3-9). Cyanidin is an aglycone of C3G which bears one hydroxyl group at C7 position of the flavonoid skeleton, while cyanidin 3,5 di-glucoside contains one anthocyanidin moiety called O-glycosidically linked to a carbohydrate moiety at the C5-position. Unique structures among C3G derivatives were assumed to affect different responses to binding activity with β_2AR. The results showed that C3G, but not cyanidin and C3,5-diGlc, potently increased CRE promoter activity in

reporter assay (Fig. 3-7) and stimulated HGF production levels in ELISA assay (Fig.3-8). These effects were shown in dose-dependent manner.

3.4. Discussion

To elucidate the molecular target of C3G on HGF stimulation, the author evaluated the promoter activity of CRE and cellular cAMP levels using HEK293 cells expressing β_2AR. C3G stimulated promoter activity of CRE and cAMP levels in dose-dependent effects. These stimulations were only detected in β_2AR-expressing HEK293 cells, indicating that C3G acted as an agonist for β_2AR to stimulate HGF production via PKA signaling pathway.

The binding of β_2AR to its agonist promotes its activation by changing conformational changes of G_s which consists of guanine nucleotide binding α subunit (Gα) and a βγ dimer (Gβγ). Upon β_2AR activation, guanosine diphosphate (GDP) is exchanged for guanosine triphosphate (GTP), promote the activation of Gα and their dissociation from Gβγ subunits, and further activate adenylyl cyclase (AC) located on the cytoplasmic side of the plasma membrane. This activation increases cAMP levels leading to PKA activation[70]. Upon activation, the PKA active molecules translocate into nucleus which further promote CREB phosphorylation. CRE has been known to bind together with phosphorylated CREB at Ser133 residue indicating the initiation of transcription of *HGF* gene[56].

In some cases, GPCRs including GPR43, GPR41, GPR109A, GPR120, and GPR40 bind to various dietary metabolites produced in the gut and transmit signals for immune and metabolic system. It has been reported that GPCRs also interact with polyphenols, as more than half of the identified polyphenol-protein interactions belong to the quercetin (2,500 interactions), coumestrol (1,802 interactions), genistein (916 interactions), trans-resveratrol (738 interactions), and acetyl-salicylic acid (510 interactions)[71]. The current study provides possibility of potential interaction of

GPCR and anthocyanidin derivative, which correlates with its beneficial effects of HGF production through cAMP- specific PKA signaling pathway.

The binding modes of β_2AR activation has been reported to be classified into full agonist, partial agonist, and biased ligand which are different among the functions of ligands[64]. Hydroxybenzyl isoproterenol (HBI) and adrenaline (epinephrine) bearing catechol groups exhibit full agonism for β_2AR[72]. Binding of full agonist causes the activation of G proteins (Gs) signaling which further binds to adenyl cyclase to stimulates cAMP as second messenger molecules for PKA activation[73]. Meanwhile, partial agonist such as salmoterol has two saligenin hydroxyl groups which also form hydrogen bond with Ser203$^{5.42}$ and Ser207$^{5.46}$ similar to epinephrine, but, compared to epinephrine, the presence of methylene between meta position of hydroxyl group and phenyl ring causes weaker effect on stabilizing the inward movement of TM5[74]. Another possible ligand interaction is biased ligand which preferably activates β–arrestin, rather than Gs signaling, such as carvediolol[75]. In this study, C3G has been demonstrated to enhance CRE promoter activity and cAMP levels in a β_2AR-dependent manner which may correlate with Gs-activated PKA pathway, thus the author indicated that C3G acted as an agonist for β_2AR.

The catechol groups in isoproterenol, epinephrine, and formoterol serve as hydrogen bond donor to Ser203$^{5.42}$ and Ser207$^{5.46}$ and cause the arrangement of TM5 and TM 3/6 in β_2AR[72]. Thus, catechol groups in C3G structure may also serve similar functions. Other functional groups found in isoproterenol and epinephrine such as secondary alcohol, amine groups, and phenol group interact with Asp113$^{3.32}$ and Asn312$^{7.39}$ which may contribute for the agonistic activity. The similar interactions may be found with the hydroxyl groups on phenyl ring of C3G. In addition, the aromatic chromane ring is found in C3G corresponding to the similar position in quercetin which has been reported to mainly stabilized by π-π interaction with an aromatic side chain of Phe290[67] (Fig 3-10).

The functional group of C3G, 3-glucoside moiety, may interact with β_2AR and contributes for the agonistic activity. Kato, E, *et al.* demonstrated that higenamine 4'-*O*-β-$_D$-glucoside, a plant-derived tetraisoquinoline compound enhanced glucose uptake in L6 cells. The presence of glucoside moiety has been discussed to exert potential function as a β_2AR binder in. In addition to glucoside moiety, the hydroxyl groups also play important role β_2AR binding because methylation of these groups can disrupt the binding activity suggesting lower importance of larger space for the methyl group in this position[31]. Based on this study, the author also assumed that the glycosylation of hydroxyl group in Cyanidin3,5-diGlucoside (C3,5-diGlc) may occupy larger area so that 5-glucoside interferes with binding activity to β_2AR, indicating that C3G exerted more potent levels of CRE activity and HGF production, compared to its aglycone and C3,5-diGlc (Fig. 3-7, 3-8).

In this chapter, the author investigated the target of C3G to activate PKA pathway as main signaling in stimulating HGF production. Given that C3G enhanced CRE promoter activity and cellular cAMP levels in β_2AR-dependent response, the author assumed that C3G targets β_2AR as an agonist. Furthermore, the author also estimated a binding site of C3G that may possess an agonism activity to β_2AR. Although further investigations such as crystal structural analysis and structure-activity relationship study are needed, this estimation suggested glucoside moiety in C3G potentially interacts with β_2AR. In conclusion, C3G increased HGF production via PKA pathway, by targeting β_2AR. In response to C3G, β_2AR undergoes conformational changes by exchanging GDP to GTP that activates adenylyl cyclase (AC), quickly converting ATP to cAMP. Elevated cAMP levels will activate protein kinase A (PKA) by dissociation of regulatory and catalytic subunits. The free catalytic subunits will be responsible for the CREB phosphorylation that binds to its promoter, CRE, to activate transcription of *HGF* gene (Fig. 3-11).

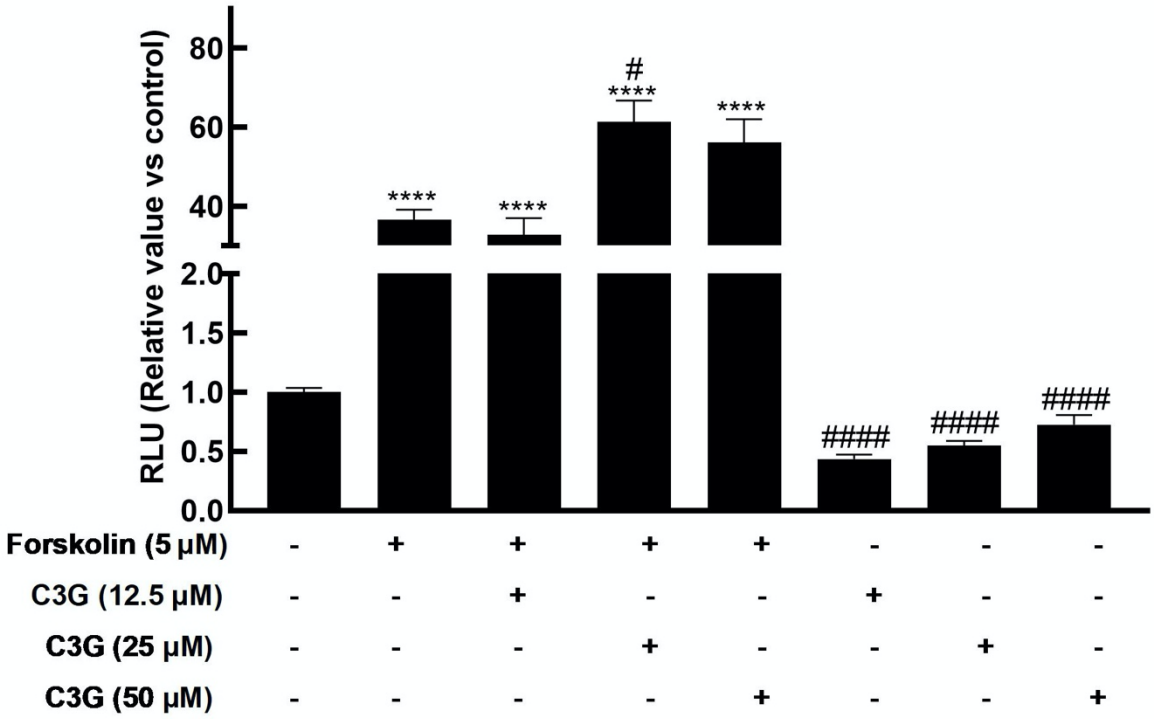

Figure 3-2. Effect of C3G on Promoter Activity of CRE. HEK293 cell were transiently transfected with pGL4.29, then seeded into 12-well plate. After overnight incubation, cells were treated with vehicle (0.1% DMSO), forskolin (5 μM), C3G (12.5, 25, or 50 μM), or combination of forskolin (5 μM) and C3G (12.5, 25, or 50 μM) for 6 h treatment. Luminescence was measured using cell lysates. Statistical analysis was conducted using one way ANOVA (Tukey's test). Significant differences ($p < 0.0001$) versus vehicle (****) or forskolin treatment group (####). Significant differences ($p < 0.05$) versus forskolin treatment group (#). n=5.

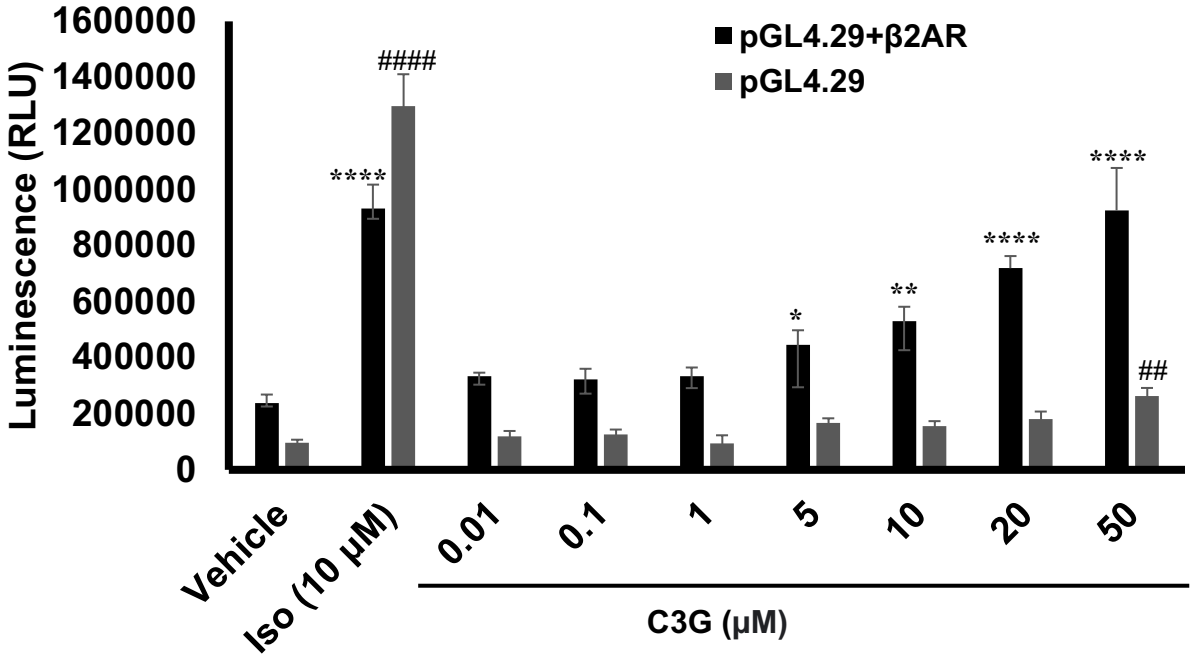

Figure 3-3. Effects of C3G on Promoter Activity of CRE in β_2AR-Co-Transfected HEK293 cells. HEK293 cell were transiently transfected either with pGL4.29 and pCDNA3.1- β_2AR, or transfected with pGL4.29 only, then seeded into 96-well plate. At the same time, cells were treated with vehicle (0.1% DMSO), Isoproterenol (10 μM, shown as Iso), C3G (0.01, 0.1, 1, 5, 10, 20, or 50 μM) for 24 h treatment. Luminescence was measured using cell lysates. Statistical analysis was conducted using one-way ANOVA (Tukey's test). Significance differences (****$p < 0.0001$, **$p < 0.01$, *$p < 0.05$) versus vehicle treatment group at cells co-transfected with pGL4.29 and pcDNA3.1-β_2AR. Significant differences (####$p < 0.0001$, ##$p < 0.01$) versus vehicle treatment group at cells transfected with pGL4.29. n = 5.

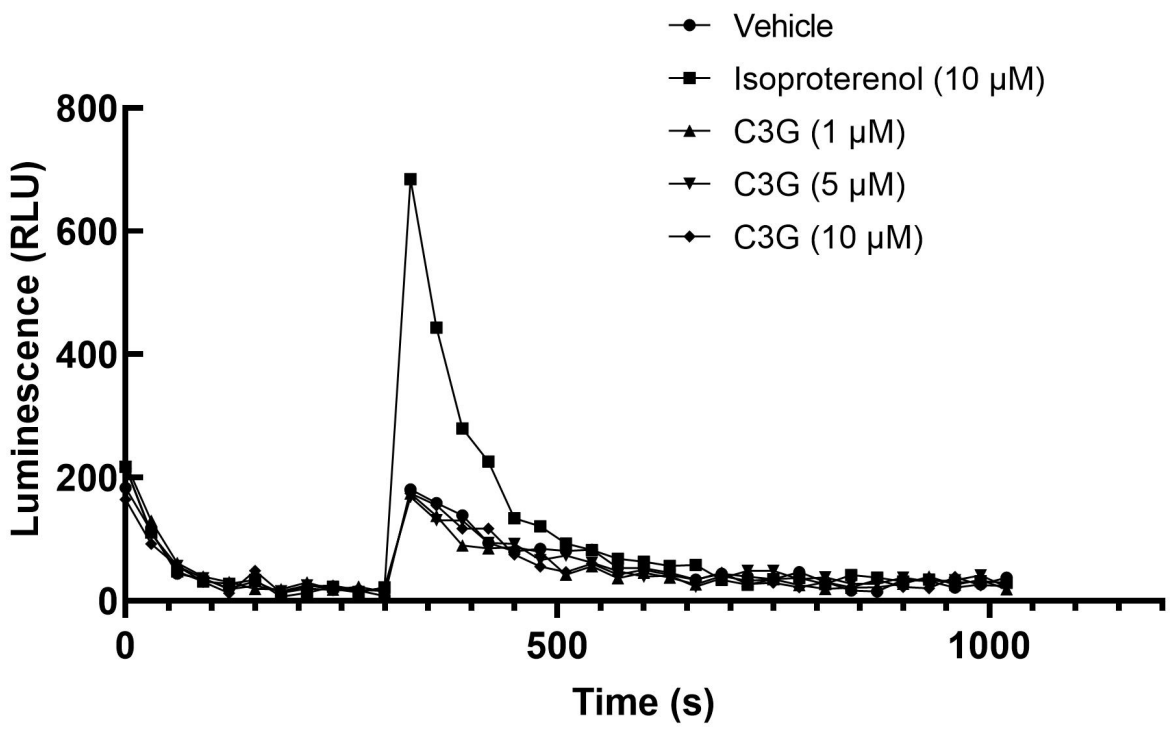

Figure 3-4. Effect of C3G on the intracellular cAMP levels in pGloSensor-22F cAMP-transfected HEK293 cells. HEK293 cell were transiently transfected with pGloSensor-22F cAMP, then seeded into 96-well plate. The cells were treated with vehicle (0.1% DMSO), Isoproterenol (10 μM), C3G (1, 5, or 10 μM) for 24 h treatment. Kinetic measurement of intracellular cAMP was measured following manufacture's protocol of GloSensor cAMP assay using micro plate reader. n = 3.

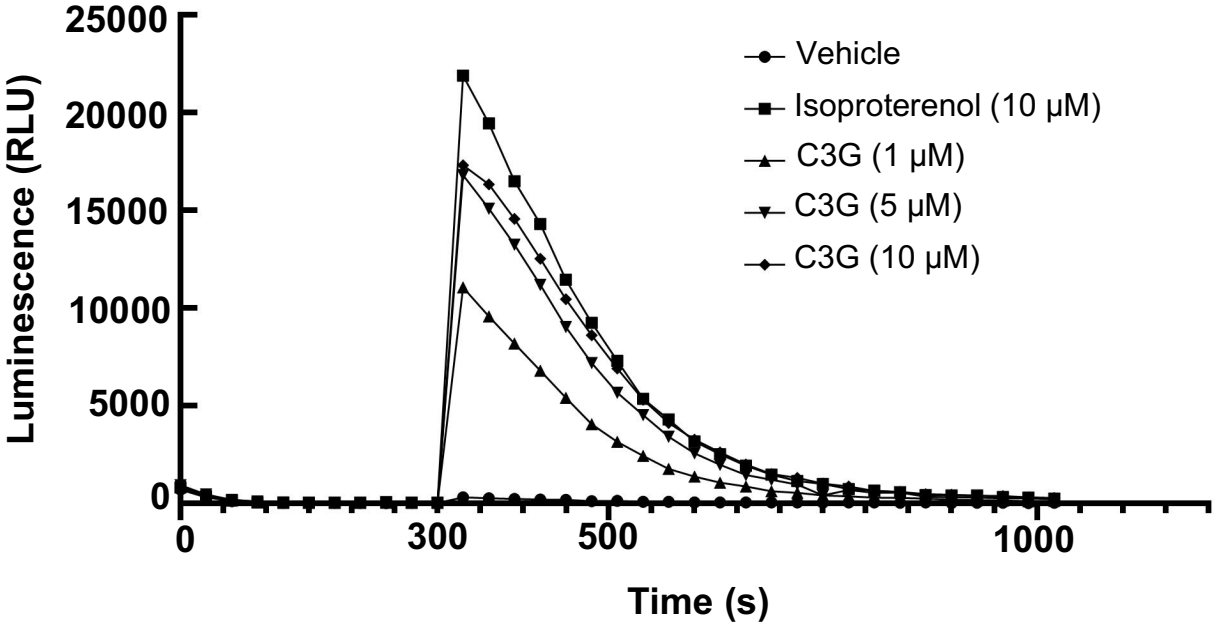

Figure 3-5. Effects of C3G treatment on the intracellular cAMP levels in pGloSensor-22F cAMP and β_2AR-co-transfected HEK293 cells. HEK293 cell were transiently co-transfected with pGloSensor-22F cAMP and pcDNA3.1- β_2AR, then seeded into 96-well plate (white). The cells were treated with vehicle (0.1% DMSO), Isoproterenol (10 μM), or C3G (1, 5, or 10 μM) for 24 h treatment. Kinetic measurement of intracellular cAMP was measured following manufacture's protocol of GloSensor cAMP assay using micro plate reader. n = 3.

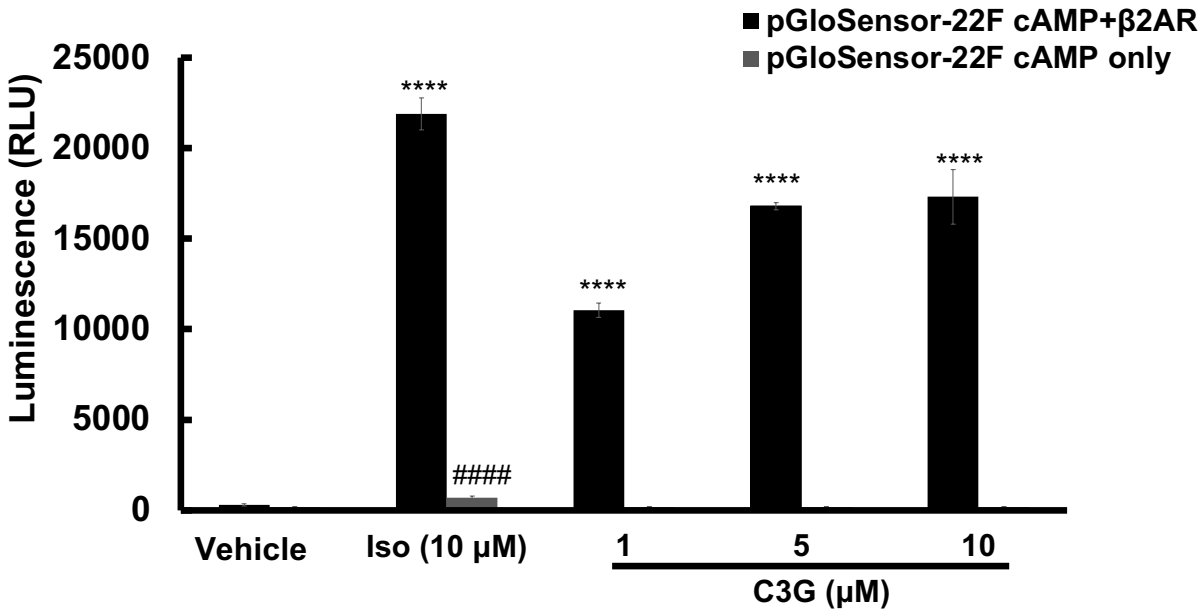

Figure 3-6. Peak value of RLU in C3G treatment on the intracellular cAMP levels in pGloSensor-22F cAMP and β_2AR-co-transfected HEK293 cells. HEK293 cells were transiently co-transfected with pGloSensor-22F cAMP and pcDNA3.1- β_2AR, then seeded into 96-well plate. Transfected cells were treated with vehicle (0.1% DMSO), isoproterenol, or C3G at the indicated concentrations, then kinetic measurement of intracellular cAMP was performed. Statistical analysis was conducted using one-way ANOVA (Tukey's test). Significant difference (****p <0.0001) versus vehicle treatment group on the cells co-transfected with pGloSensor-22F cAMP and pcDNA3.1- β_2AR. Significant difference (####p <0.0001) versus vehicle treatment group on the cells transfected with pGloSensor-22F cAMP. n = 3. Iso: isoproterenol (10 μM).

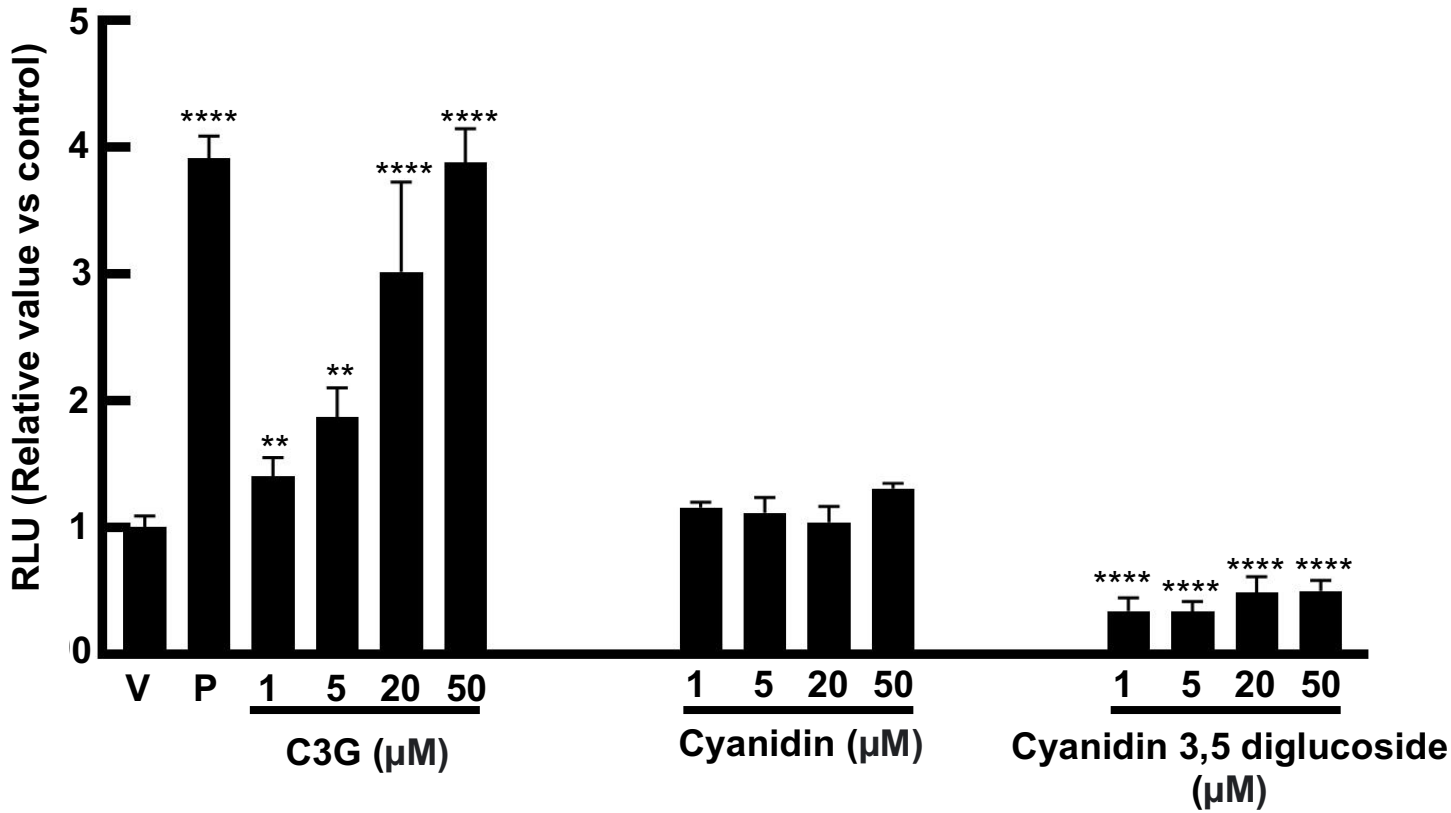

Figure 3-7. Structure-activity study of C3G and its chemical derivatives on promoter activity of CRE in β_2AR-co-transfected HEK293 cells. HEK293 cell were transiently transfected with pGL4.29 and pCDNA3.1-β_2AR, then seeded into 96-well plate. The cells were treated with vehicle (0.1% DMSO, shown as V), PDGF-BB (25 ng/ml, shown as P), C3G, cyanidin, and cyanidin 3,5diglucoside at the indicated concentrations for 24 h. Luminescence was measured using cell lysates. Statistical analysis was conducted using one-way ANOVA (Tukey's test). Significance difference (****$p < 0.0001$, **$p < 0.01$) versus vehicle treatment group. n = 5.

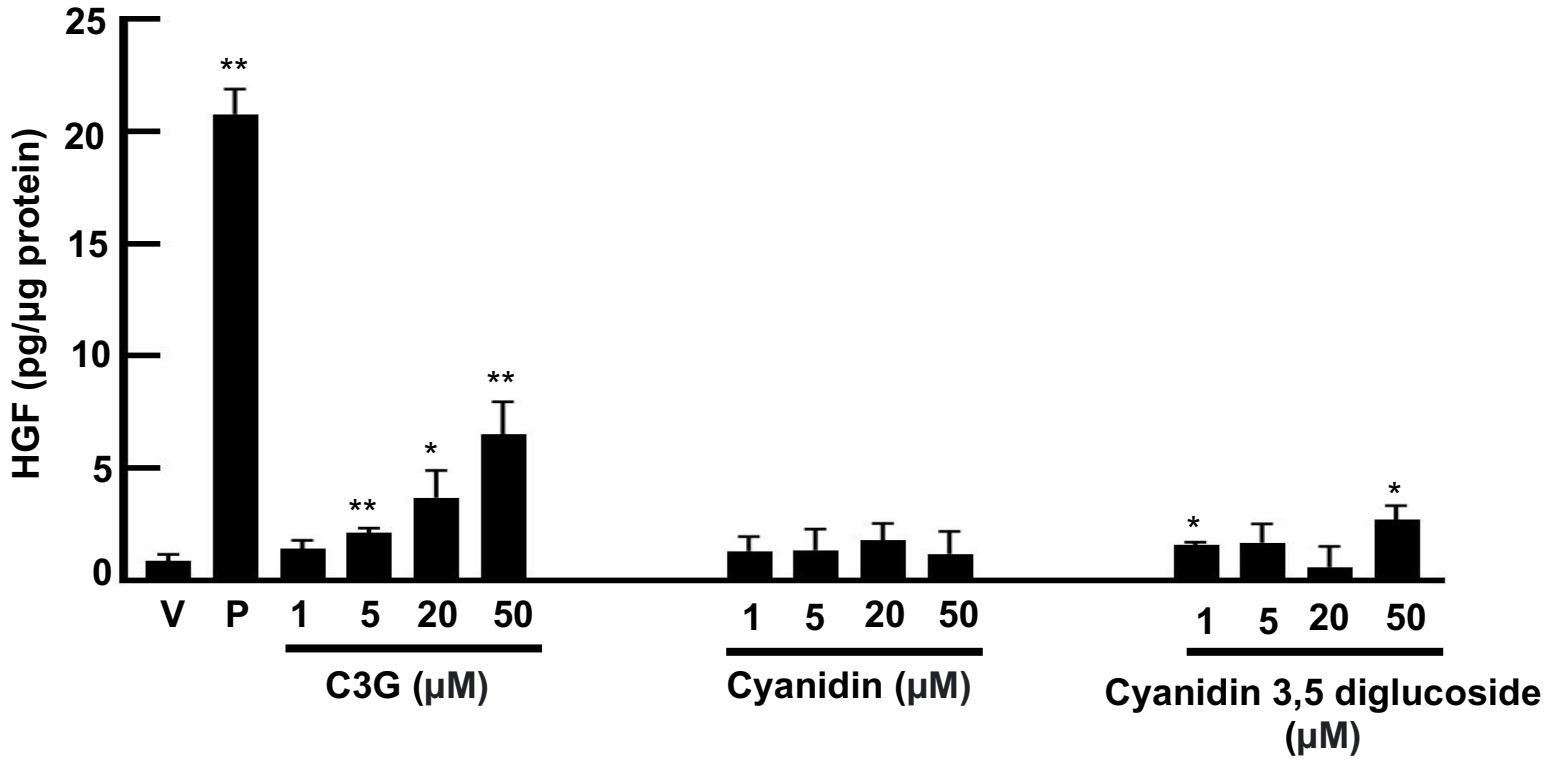

Figure 3-8. Structure-activity relationship of C3G and its chemical derivatives on HGF production in NHDF cells. NHDF cells were seeded into 96-well plate until reaching 80% confluent. The cells were treated with vehicle (0.1% DMSO, shown as V), PDGF-BB (25 ng/ml, shown as P), C3G, cyanidin, and cyanidin 3,5diglucoside at the indicated concentrations for 120 h. Total HGF levels were quantified by ELISA assay and calculated as final unit (pg/µg protein) after normalization with total protein concentrations. Statistical analysis was conducted using Student's *t*-test. Significance difference (**$p < 0.01$, *$p < 0.05$) versus vehicle treatment group. n = 5

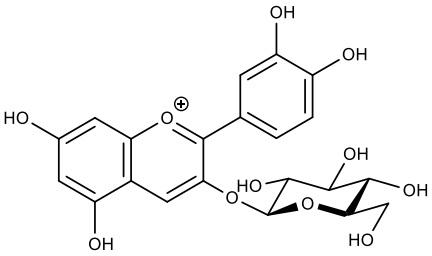

Cyanidin 3-glucoside

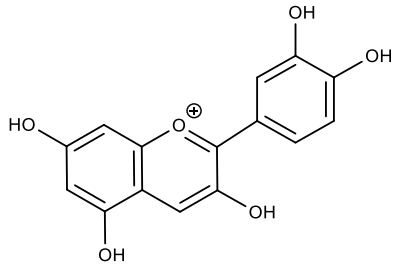

Cyanidin

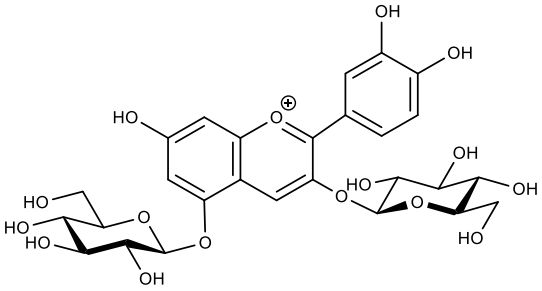

Cyanidin 3,5-diglucoside

Figure 3-9. Chemical structures of C3G, Cyanidin, and Cyanidin 3,5-diglucoside.

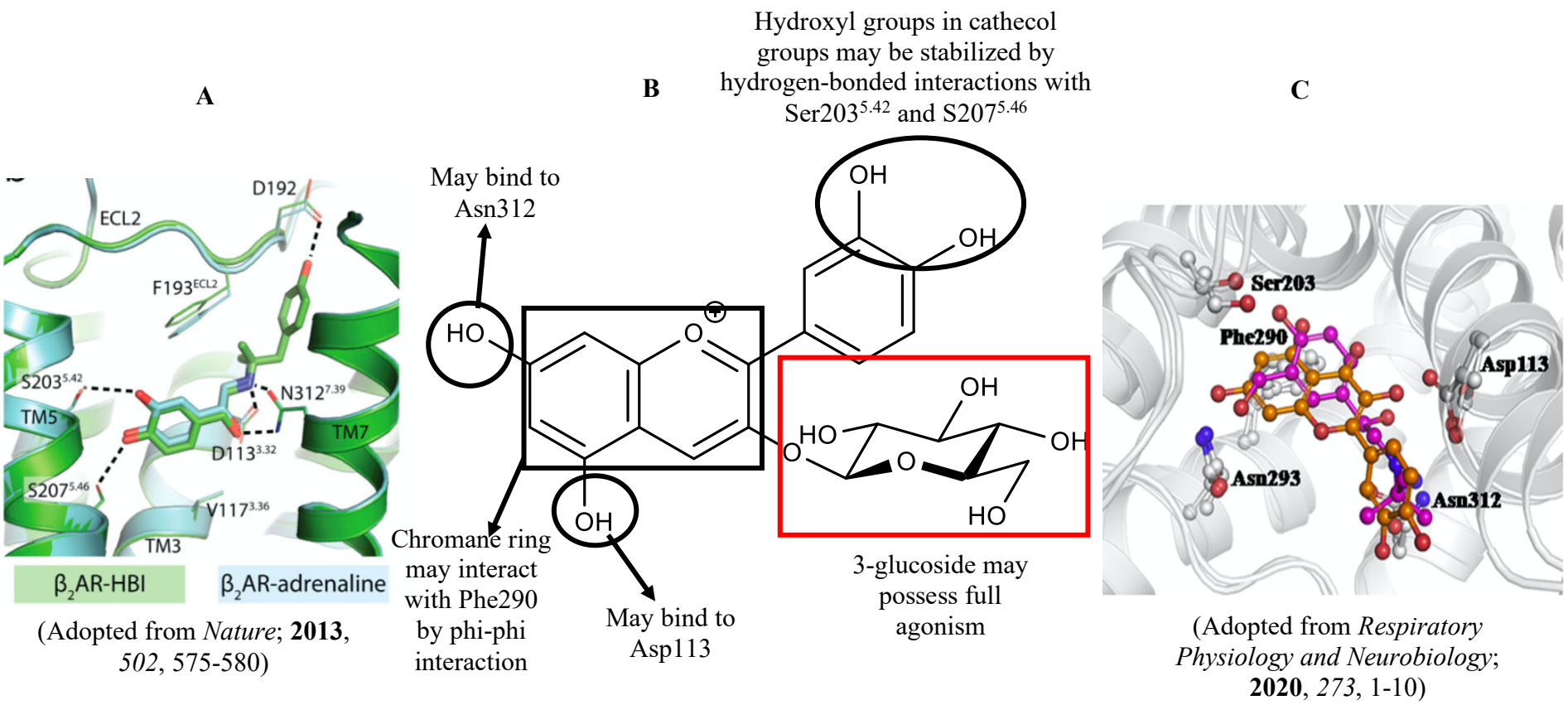

(Adopted from *Nature*; **2013**, *502*, 575-580)

(Adopted from *Respiratory Physiology and Neurobiology*; **2020**, *273*, 1-10)

Figure 3-10. Estimation of interaction between C3G and β$_2$AR. Binding mode of hydroxybenzyl isoproterenol (HBI) (green) and adrenaline (blue) in β$_2$AR (A) (Adopted from *Nature*; **2013**, *502*, 575-580). Possible interaction of C3G with β$_2$AR (B). Binding modes of quercetin (orange) and salbutamol (magenta) in β$_2$AR (C) (Adopted from *Respiratory Physiology and Neurobiology*; **2020**, *273*, 1-10).

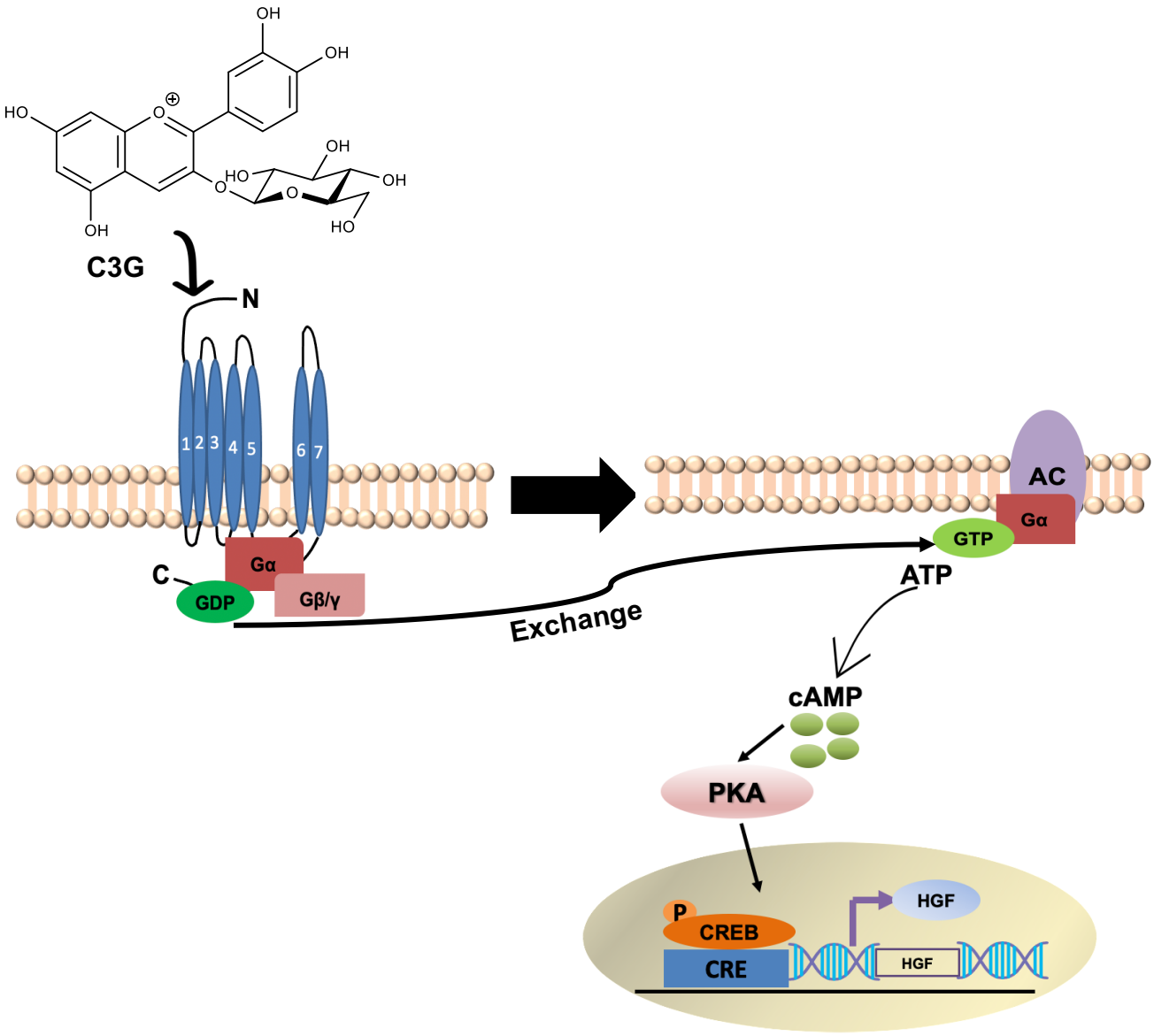

Figure 3-11. Schematic diagram of the mechanisms of C3G in stimulating HGF production through PKA pathway by targeting β_2AR. C3G increased HGF production via PKA pathway, by targeting β_2AR. In response to C3G, β_2AR undergoes conformational changes by exchanging GDP to GTP that activates adenylyl cyclase (AC), then quickly converting ATP to cAMP. Elevated cAMP levels will activate protein kinase A (PKA) which is responsible for the CREB phosphorylation that binds to its promoter, CRE, to activate transcription of *HGF* gene.

Chapter 4

HMOs may prevent HUVECs growth in the presence of TNF-α in the co-culture system

4.1 Introduction

The main functions of growth factor to regulate numerous signaling cascades in many cellular processes including cell proliferation, migration, differentiation, and multicellular morphogenesis during tissue healing and development are triggered initially by a specific ligand binding toward the interaction between growth factors and their specific cell surface receptor[4, 76]. Many studies have been conducted to provide critical roles of HGF- *c*-Met pathways in regulating cellular processes. The investigations of food-derived components as growth factor inducers are essential to evaluate these critical roles. In Chapter 2, the author showed that C3G is potential to stimulate HGF production levels from upstream signaling pathway. As an HGF inducer, C3G activated β_2AR signaling pathway leading to promote cAMP- specific PKA pathway which then activate transcriptional activity of *HGF* gene. This investigation support other studies showing elevation levels of HGF become therapeutic potential in modulating dynamic morphogenesis, tissue regeneration, and cell survival in hepatocytes, renal tubular cells, and neuronal cells.

However, overactivation of signaling cascades triggered by growth factors resulting from gene amplification, chromosomal translocation, and mutations of growth factors and their receptors causes alterations leading to multistep of cancer development such as angiogenesis, invasion, and metastasis[77]. Overactivation of growth factor such as VEGF which is expressed in vascular endothelial cells is a key mediator of angiogenesis. This cellular process could support good environment for cancer development and growth. In Chapter 4, the author investigated the effects of Human Milk Oligosaccharides (HMOs) on the overactivation of VEGF induced by TNF-α-modulated inflammation by observing HUVECs morphology as the outcome of angiogenesis process.

One of the food components are known as HMOs have been attracted great attention among researcher as it is considered as a potential novel food due to its unique oligosaccharide structure and composition. Comparing to other oligosaccharides in other mammalian's milk, such as cow's milk, HMOs are unique as their abundance in structural variety and concentrations in milk. Initially, isolation and purification of HMOs directly from human milk were difficult, but it has been successfully conducted by the discovery of new technology such as chemical synthesis and fermentation technology. The discovery of these methodologies was able to generate several simple structures such as 2'FL, 3'SL, 6'SL and LNnT which then triggers researchers to explore their biological functions. In this study, the author investigated the potential roles of HMOs in the regulation of HUVEs morphology that is correlated to angiogenesis-like morphology.

Angiogenesis is a normal and complex process that involves endothelial cell activation by endogenous local or systemic chemical signals. Angiogenesis is needed for physiological process during embryo development, wound healing, and collateral formation for improved organ perfusion. However, abnormal accelerated angiogenesis is associated with pathological conditions which trigger various disorders including tumor development-related neovascularization. Current angiogenesis inhibitors as anti-angiogenesis in cancer therapy are not effective in humans since they only halt the growth of tumors, not eliminate. In addition, angiogenesis inhibitors may potentially disturb many normal body processes such as wound healing, blood pressure, kidney function, and so on[78]. Thus, the search for anti-angiogenic compounds from natural sources is still needed, particularly a promising compound with various actions to target VEGF and its receptors (VEGFR), as a powerful angiogenic agent in neoplastic vascularization[79].

Caco-2 cells derived from human colon adenocarcinoma, have been found as a good model for intestinal epithelial cells because they are able to exhibit various enterocytes characteristics

including brush-border enzymes, nutrient transporter activities, and tight junctions, once they are differentiated during culture on semipermeable membrane. The author performed co-culture Caco-2 and HUVECs to observe the inhibitory effects of HMOs on HUVEC's growth in the presence of TNF-α which stimulates VEGF production from Caco-2. A report showed co-culturing Caco-2 and human endothelial cell line (EA.hy926) with TNF-α (10 ng/ml) exhibited inflammation like changes. The exposure to TNF-α modulated the expression of 400 genes in endothelial cells related to cell adhesion, inflammation, and chemotaxis. The expression levels of VEGF, NO, and ROS were significantly increased in the co-culture system[80]. This co-culture system is an intriguing approach to observe the effects of HMOs in inhibiting TNF-α-induced VEGF secreted from Caco-2 cells.

The study of specific effects of HMOs as anti-angiogenesis is still limited, thus further experiments are needed to investigate the beneficial functions of HMOs, for anti-angiogenesis. Therefore, the author conducted *in vitro* study by using HUVECs to investigate the effects of HMOs, particularly on HUVEC's viability in the presence of VEGF. This study also described another example of food-derived components to suppress the effects of growth factor to provide beneficial effects in such of disease treatment in the future.

4.2 Materials and methods

4.2.1 Human Milk Oligosaccharides (HMO)

HMO powder samples (fucosyllactose; 2'-FL, sialyllactose; 3'-SL and 6'-SL, and lacto-n-neotetraose (LnNT)) were provided by Kyowa Hakko Bio Co., Ltd. HMO stock solutions (100 mM) were prepared by dissolving HMOs in PBS as much as 5 mL, then filtered using a syringe equipped with microfilter (Millex Filter Unit, 0.22 μM) into 2 mL of screw cap tubes (1 mL stock solution in each tube). The stocks were kept in the -20^{o}C freezer. HMOs' weight was calculated based on the molecular weight as Table 1.

4.2.2 Cell lines and cell cultures

Human umbilical vascular endothelial cells (HUVECs) were obtained from Lonza. HUVECs were cultured in endothelial cells basal medium 2 (ECBM 2) with SupplementPack containing fetal calf serum, epidermal growth factor, basic fibroblast growth factor, insulin-like growth factor, vascular endothelial growth factor 165 (VEGF), ascorbic acid, heparin, and hydrocortisone (Promo Cell). Caco-2 cells, provided from Prof. Isoda, were cultured in Dulbecco's Modified Eagle's Medium, high glucose, GlutaMax supplement (Gibco #10566016) supplemented with 10% fetal bovine serum (Gibco^{TM}) and 1% antibiotic (5000 U/mL penicillin and 5000 μg/mL streptomycin) (Lonza).

All cells used in this experiment were incubated at 37^{o}C in a humidified 95% air, 5% CO_2 atmosphere.

4.2.3 Caco-2 cell differentiation

Firstly, Caco-2 cells were maintained in 75 cm^2 culture flask until they become confluent. The medium was changed twice a week. After density become confluent, the cells were subcultured and continuously cultured for 14 days in transwell 12-well cell culture insert with 0.4

μm semipermeable support membrane (Corning-Costar, Bedford, USA). The cell density was $1x10^5$ cells/1.12 cm^2 insert. A half milliliter of a medium was placed in the insert (apical side) and 1.5 ml of the same medium was placed in the lower side (basolateral side). The medium was replaced twice a week.

4.2.4 Co-culture of Caco-2 and HUVECs and measurements

HUVECs were cultured in the 12-well plate for 24 h. On the next day after the cells were attached well, differentiated Caco-2 cells which were placed on Transwell insert membrane were cultured on the HUVEC wells as shown in Fig. 4-1. The old medium was replaced with the 0.5 mL of fresh medium with or without 1 mM HMOs at the apical side and 1.5 mL ECBM-2 at the basolateral side for HUVECs. Negative control in this culture used ECBM-2 without VEGF and other growth factors. After HUVECs were cultured in the 12-well plate for 24 h, the old medium was removed and TNF-α supplemented medium was added into apical side. At the same time, HMOs at 2 mM were added to the apical side.

4.2.5 Lactate Dehydrogenase (LDH) assay

After culturing Caco-2 and HUVECs in 12-well plate for 14 days and 1 day, respectively, Caco-2 inserts were placed on the HUVECs wells, then the Caco-2 cells were treated with 10 ng/ml TNF-α, HMOs (2 mM) or co-treatment of TNF-α and HMOs at the same time to the apical membrane. The LDH assay was performed in day 5 incubation based on the protocol from the manufacturer (LDH assay kit (colorimetric), Abcam #ab65393). The microscopic observation was done on day 5 incubation.

4.2.6 Scratch assay

After culturing Caco-2 and HUVECs in 12-well plate for 14 days and 1 day, respectively, the HUVECs was in 60% confluent. The HUVECs were scratched with a 10-200 scratched with a 10–200 μL pipette tip (yellow tip) to make a straight line on the HUVEC monolayer. After that, Caco-2 inserts were placed on the HUVECs wells. At the same time, the Caco-2 cells were treated with TNF-α (10 ng/ml), mix HMOs (2 mM), or co-treatment of TNF-α and HMOs at the same time to the apical membrane (Fig. 4-2a). The cell morphology was observed under microscope until day 5. To make comparison, HUVECs were also cultured alone before scratch assay was done (Fig. 4-2b).

4.2.7 Tube formation assay

Tube formation assay was done based on the method previously reported (Chung et al., 2017) with modification. Briefly, HUVECs were seeded on the Matrigel-coated wells (BD Bioscience, San Jose, CA, USA). Then, HUVECs were incubated for 24 h to form the tubular morphology. When the tube formations have been formed, the old medium of ECGM-2 was replaced with free serum ECGM-2 medium. After that, Caco-2 cells were placed on the HUVECs cultured on Matrigel coated wells which then were treated with TNF-α (10 ng/ml), mix HMOs (2 mM), or co-treatment of TNF-α and HMOs at the same time to the apical membrane (Fig. 4-3a). The cell morphology was observed under microscope until day 3. To make comparison, HUVECs were also cultured alone before tube formation assay was done (Fig. 4-3b).

4.3 Results

4.3.1 Effects of HMOs on HUVECs morphology co-cultured with TNF-α-treated Caco-2 cells

After 5 days incubation, HUVECs morphology was observed under microscope and the author found that HUVECs cell debris in positive control (Caco-2 cells were treated with TNF-α) seemed to be much lower than negative control (Caco-2 cells were treated in medium without VEGF). Interestingly, the author also found HUVECs cell debris seemed to be much higher in the co-treatment of TNF-α and HMOs, compared to other groups (Fig. 4-4a). To confirm with quantitative data, the author performed LDH assay (Fig. 4-4b) and found that combination TNF-α and HMOs-treated Caco-2 cells showed significantly higher LDH levels which was indicated by the presence of cell debris of HUVECs.

4.3.2 Effects of HMOs on HUVECs growth co-cultured with TNF-α-treated Caco-2 cells by scratch assay

Compared to HUVECs grew in VEGF-free medium (Fig. 4-5a), HUVECs grew in co-culture did not migrate and proliferate, but they survived (Fig. 4-5b). The author assumed that co-culture system maintained HUVECs survival (viability). HUVECs cultured alone did not survive shown by abundant cell debris on the surface of the culture medium, assuming Caco-2 cells may secrete growth factors that stimulate HUVECs survival. The addition of TNF- α induced the migration of HUVECs, but HUVECs also did not migrate in the treatment of mixed HMOs and the combination of TNF-α (Fig. 4-5b).

4.3.3 Effects of HMOs on HUVECs growth co-cultured with TNF-α-treated Caco-2 cells by tube formation assay

During Matrigel application for 5 hours before treatment, the author has confirmed that tube formation is well formed in all wells (Fig. 4-6a). Afterwards, the author conducted treatments and observed the tube formation under microscope after 3-days incubation. HUVECs co-cultured with Caco-2 seemed to maintain tube and branch formation better, compared to HUVECs cultured alone without VEGF (Fig. 4-6b). TNF- α treatment in co-culture Caco-2 and HUVECs seemed to maintain tube and branch formation well, compared to HUVECs treated with the combination of TNF-α and HMOs (Fig. 4-6b).

4.4. Discussion

In this study, the author investigated the modulation effects of HMOs on TNF-α-induced VEGF in HUVECs morphology co-cultured with Caco-2 cells. HUVECs have been known as a good model of cell culture to study angiogenesis because it was reported that miRNA expression in HUVECs showed highly expressed the receptors of angiogenic factors as putative targets[81]. Additionally, the author performed TNF-α-treated Caco-2 cells co-cultured with HUVECs. The author performed initial investigation by observing HUVECs morphology in day 5 incubation and found the HUVECs viability in co-culture system with Caco-2 was better than HUVECs cultured alone. TNF-α may increase one of the HUVECs' growth factors, such as VEGF. The evident effects of TNF-α-induced VEGF may be the outcome of inflammation-like signaling from Caco-2 stimulated by TNF-α. These results may correlate with a review study which stated that TNF-α is known as a proinflammatory cytokine which is critical for maintaining the intestinal integrity, and also for pathogenesis of intestinal inflammation. *In vivo* mice study showed that in the gut,

TNF-α is produced by several cells including intestinal epithelial cells and immune cells called Paneth cells during chronic inflammation. Moreover, patients suffering from chronic intestinal inflammation showed elevated levels of TNF-α due to the elevated numbers of TNF-α secreting cells in the intestine[82]. These results showed HUVECs' viability was maintained well in the presence of TNF-α added to the upper side which may be related to the increased level of VEGF by TNF-α and this effect was diminished by HMOs at 2 mM indicated by cell debris was formed in culture.

Angiogenesis is indicated of the step for endothelial cells to form capillary-like structure in response to angiogenic signal found in conditioned medium. Furthermore, endothelial cells also migrate into the surrounding tissue in response to angiogenic chemokines[83, 84]. To investigate the effects of HMOs on angiogenesis-like morphology in TNF-α-treated Caco-2 cells co-cultured with HUVECs, the author performed scratch assay and tube formation assay. The author found that co-treatment of HMOs and TNF-α suppressed the HUVECs migration and tube formation, compared to those treated with TNF-α. The author assumed that HMOs may suppress angiogenesis-like morphology in the presence of TNF-α-induced VEGF in HUVECs co-cultured with Caco-2 cells, indicating that HMOs may be potential as therapeutic agent in the treatment of angiogenesis, particularly involved in tumorigenesis state.

Further investigations should be performed to measure the actual level of VEGF secreted from Caco-2 cells after treatment with or without TNF-α and conduct further experiments to identify which HMO has the inhibitory effects, in addition as found in mixed HMOs in this study. Besides, analysis of HUVECs' markers (von Willebrand factor, vWf) and apoptosis assay should be done to understand the mechanisms of this effects. Furthermore, gene expression analysis in the co-culture

system may also be important to do in the future to reveal the interaction between TNF-α and VEGF in supporting HUVEC's viability, as well as how HMOs inhibit these effects.

Table 1. Molecular weights of HMOs.

HMOs Sample	Molecular Weight (g/mol)
2’FL	488.44
3’SL	655.53
6’SL	655.53
LNnT	707.63
Sialic acid	345.27

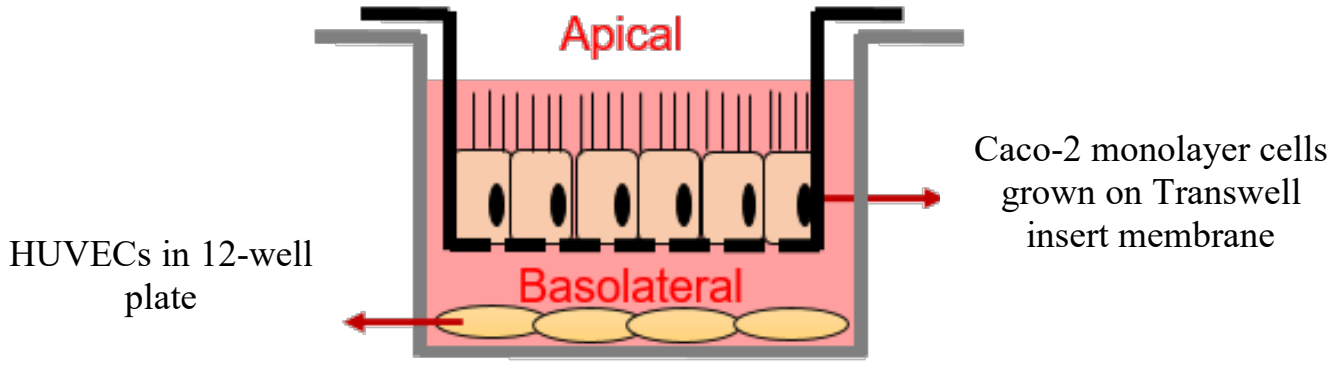

Figure 4-1. Co-culture of Caco-2 and HUVECs in 12-well plate. HUVECs were co-cultured with differentiated Caco-2 cells which were placed on Transwell insert membrane.

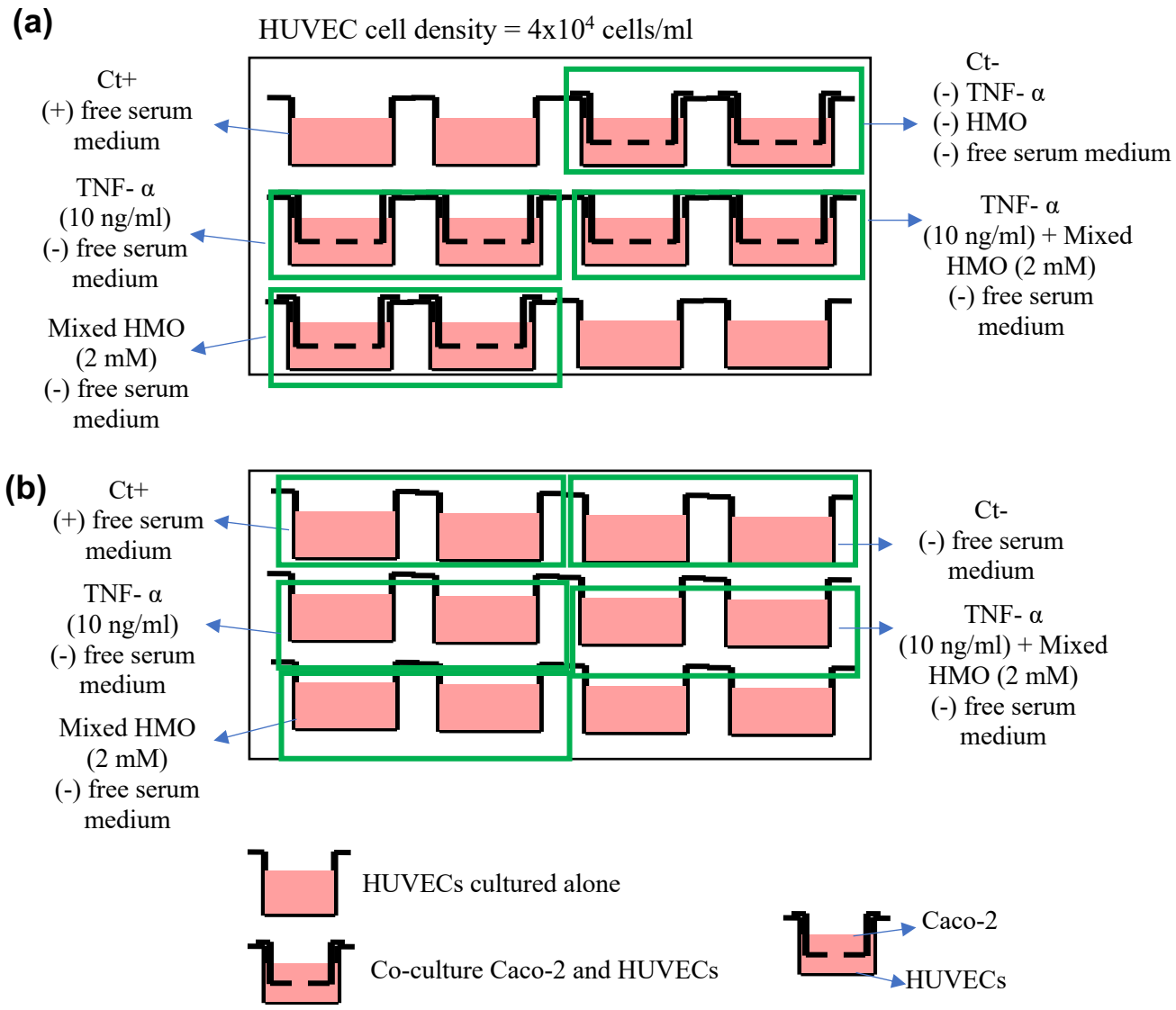

Figure 4-2. (a) Plate layout of co-culture Caco-2 and HUVECs, and (b) HUVECs cultured alone for scratch assay. The scratched HUVECs were co-cultured with differentiated Caco-2 cells which were placed on the apical membrane. At the same time, the Caco-2 cells were treated with TNF-α (10 ng/ml), mix HMOs (2 mM), or co-treatment of TNF-α and HMOs at the same time to the apical membrane. The cell morphology was observed under microscope until day 5 (a). To make comparison, HUVECs were also cultured alone before scratch assay was done (b).

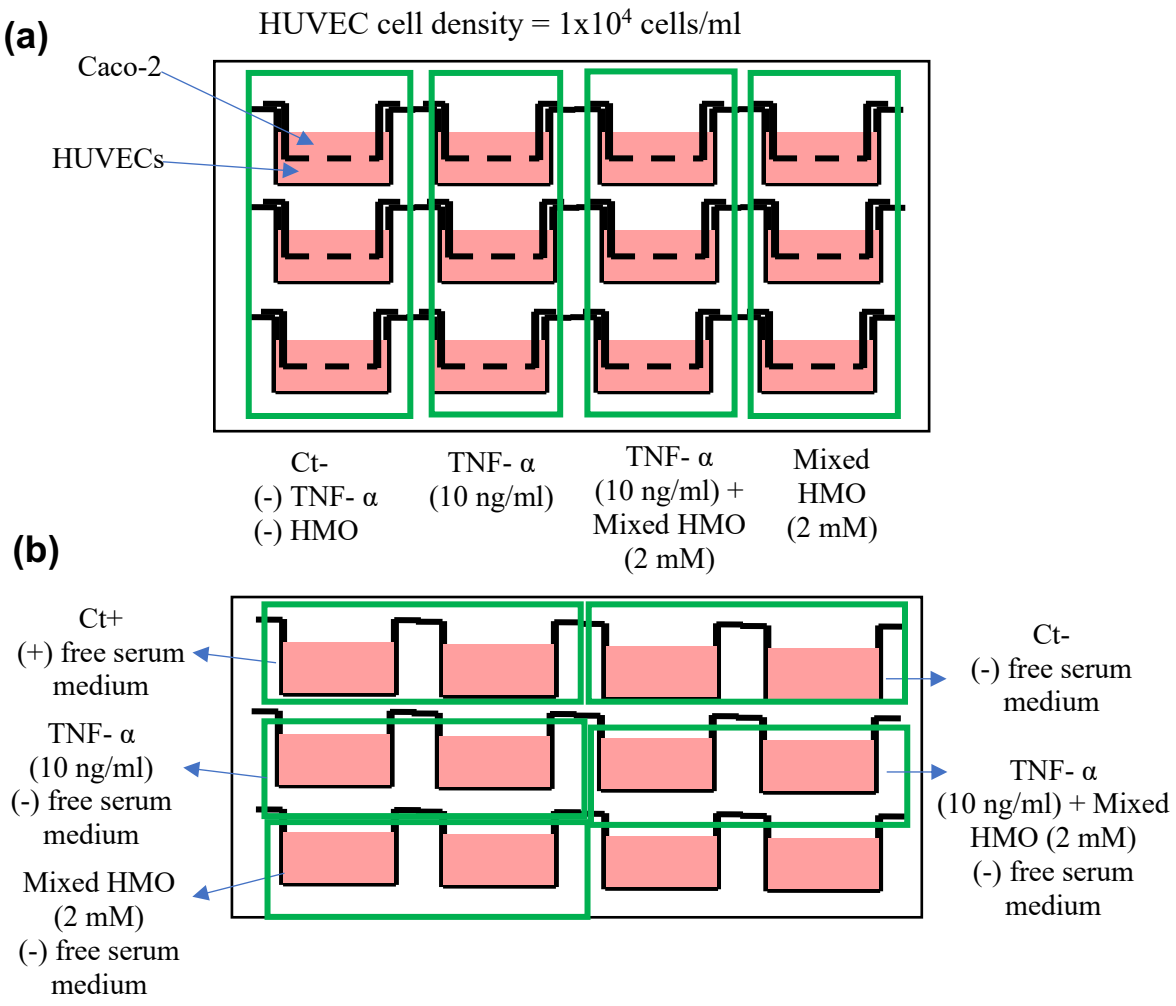

Figure 4-3. (a) Plate layout of co-culture Caco-2 and HUVECs, and (b) HUVECs cultured alone for tube formation assay. HUVECs were seeded on the Matrigel-coated wells (BD Bioscience, San Jose, CA, USA). Then, HUVECs were incubated for 24 h to form the tubular morphology. After that, HUVECs were co-cultured with differentiated Caco-2 cells which were placed on Transwell insert membrane. At the same time, Caco-2 cells were treated with TNF-α (10 ng/ml), mix HMOs (2 mM), or co-treatment of TNF-α and HMOs at the same time to the apical membrane. The cell morphology was observed under microscope until day 3 (a). To make comparison, HUVECs were also cultured alone before tube formation assay was done (b).

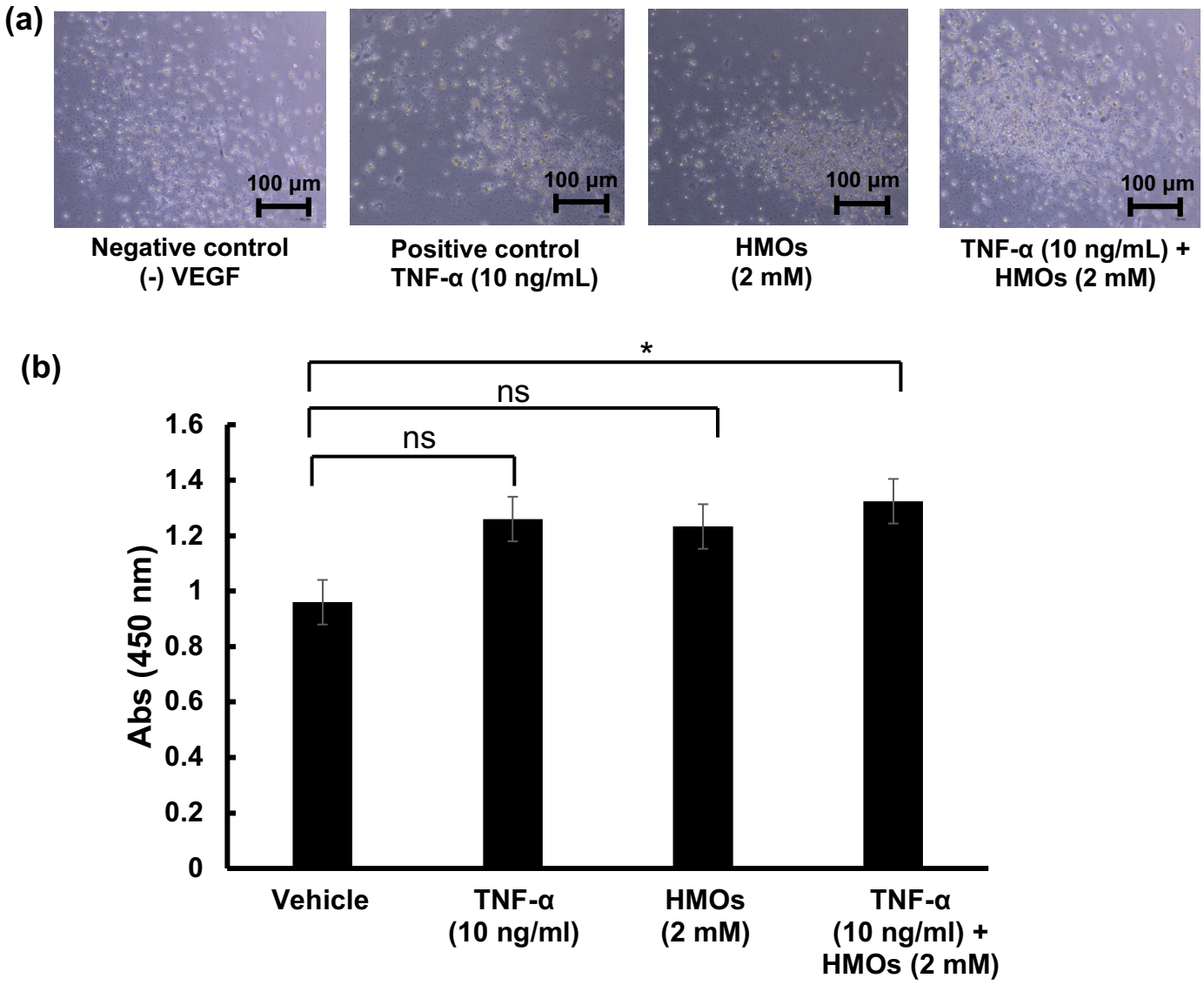

Figure 4-4. (a) HUVECs morphology in day 5 incubation; (b) LDH assay on HUVECs in day 5 incubation. After culturing Caco-2 and HUVECs in 12-well plate for 14 days and 1 day, respectively, Caco-2 inserts were placed on the HUVECs wells, then the Caco-2 cells were treated with TNF-α (10 ng/ml), HMOs (2 mM) or co-treatment of TNF-α and Mix HMOs at the same time to the apical membrane. The LDH assay was performed in day 5 incubation based on the protocol from the manufacturer (LDH assay kit (colorimetric) abcam). The microscopic observation was done on day 5 incubation. Statistical analysis was conducted using T-test analysis with statistical significance, regarded at : * significance difference, $p<0.05$ vs DMSO groups, n=3.

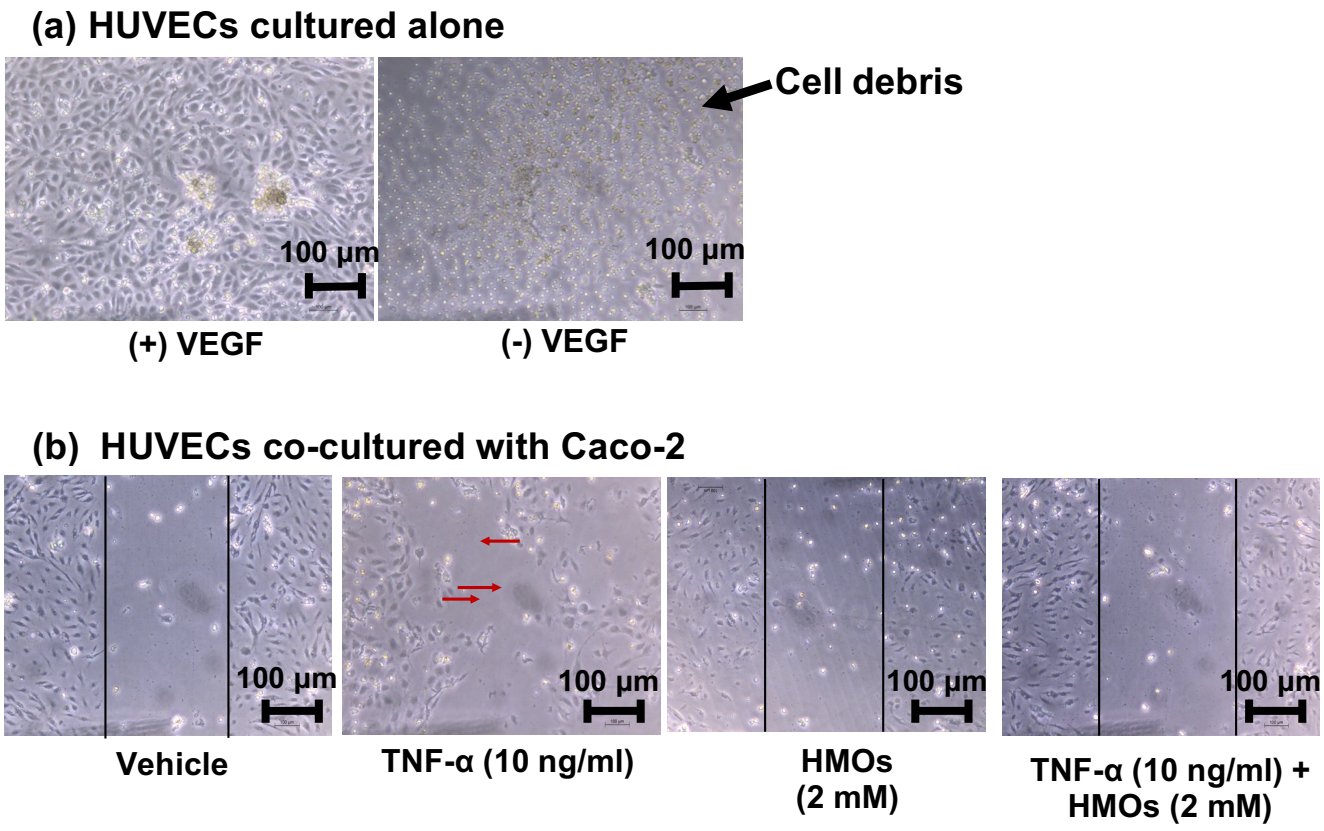

Figure 4-5. (a) HUVECs cultured alone with or without VEGF after 3 days scratch assay; (b) HUVECs co-cultured with Caco-2 cells after 3 days scratch assay. After culturing Caco-2 and HUVECs in 12-well plate for 14 days and 1 day, respectively, the HUVECs was in 60% confluent. The HUVECs were scratched with a 10-200 scratched with a 10–200 µL pipette tip (yellow tip) to make a straight line on the HUVEC monolayer. After that, Caco-2 inserts were placed on the HUVECs wells. At the same time, the Caco-2 cells were treated with TNF-α (10 ng/ml), HMOs (2 mM), or co-treatment of TNF-α and Mix HMOs at the same time to the apical membrane. The cell morphology was observed under microscope until day 5.

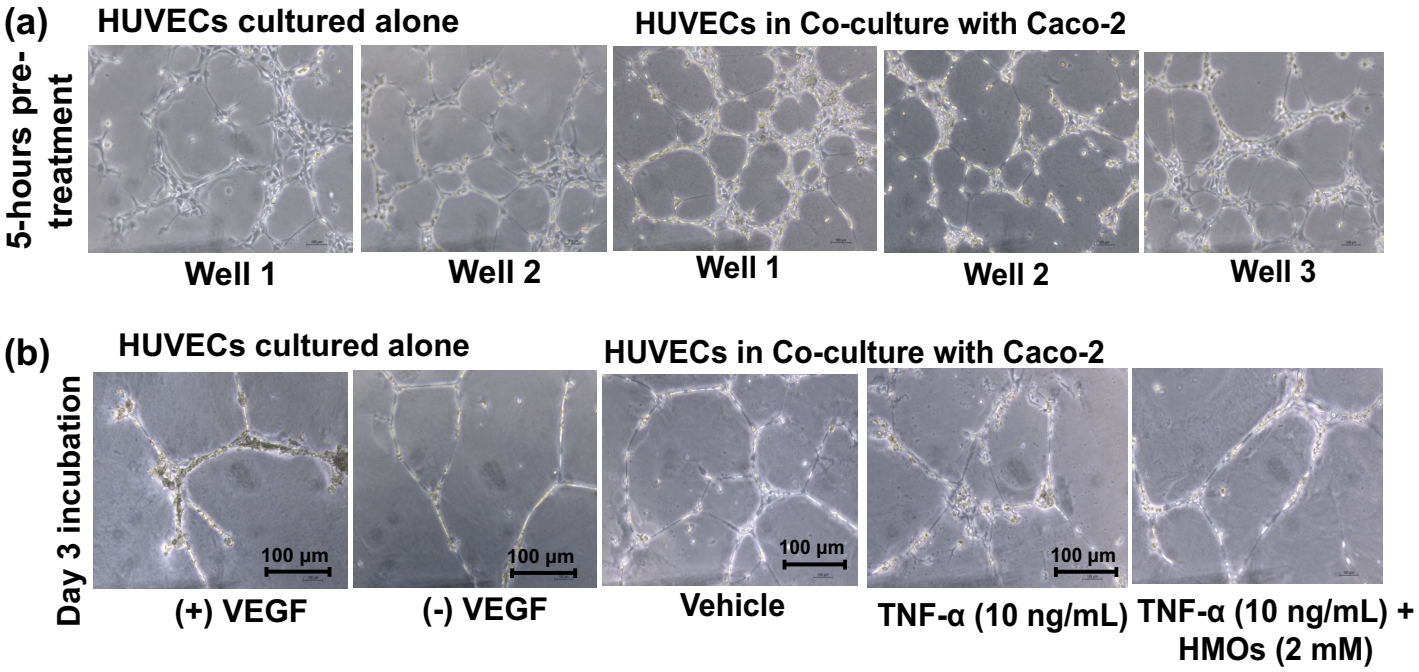

Figure 4-6. (a) HUVECs cultured on Matrigel after 5 hours incubation; (b) Tube formation observed after 3-day incubation with different treatments. HUVECs were seeded on the Matrigel-coated wells (BD Bioscience, San Jose, CA, USA). Then, HUVECs were incubated for 24 h to reach t the completion of tube formation. When the tube formations have been formed, the old medium of ECGM-2 was replaced with free serum ECGM-2 medium. After that, Caco-2 cells inserted were placed on the HUVECs cultured on Matrigel coated wells which then were treated with TNF-α (10 ng/ml), HMOs (2 mM), or co-treatment of TNF-α and Mix HMOs at the same time to the apical membrane The cell morphology was observed under microscope until day 3. To make comparison, HUVECs were also cultured alone before scratch assay was done.

Chapter 5

General Discussion

The implementation of food-derived compounds in the modulation of several growth factors such as TGF-β1, FGF, and EGF through downstream signaling have been well studied. However, alternative approach to regulate growth factors is to modulate their production in upstream signaling pathway. This mechanism controls or modulates more effectively various downstream signaling regulated by growth factor, itself, rather than regulating only specific downstream pathway. These studies suggested that food-derived compounds such as C3G and HMOs are beneficial in term of their efficacy to modulate growth factor production. Based on this motivation, this study was aimed to investigate food-derived components in modulating growth factors through upstream signaling which is comprised into three parts; 1. The investigations of C3G on HGF production in NHDF cells and its mechanisms of actions; 2. The estimation target of C3G in stimulating HGF via PKA signaling; 3. The investigations of HMOs on the modulation of angiogenesis-like morphology in TNF-α-treated Caco-2 cells co-cultured with HUVECs.

In chapter 2 and 3, the author found that C3G potently stimulated HGF production in NHDF cells by targeting β_2AR via PKA signaling pathway. The author also estimated binding site of C3G with β_2AR. C3G which is the major anthocyanin derivatives has been investigated its roles to promote cellular mechanisms through various signaling pathways, but the effects of C3G on growth factor production have not been investigated. The investigation of HGF inducers, particularly derived from natural products, has become an issue to explore the functions of HGF as a novel therapeutic agent. Based on the ELISA results, C3G strongly enhanced HGF production in dose- and time- dependent manner via PKA pathway, which was suppressed in the presence of PKA pathway inhibitors. The mechanisms of actions on HGF productions by C3G were also investigated. C3G was found to target β_2AR to activate PKA pathway, including increase of intracellular cAMP levels, activation of phosphorylated CREB, and finally induction of CRE

promoter activity to further trigger the transcription of HGF, as a target gene. The cathecol groups, aromatic chromane ring, and phenyl ring which is found similarly in C3G and its derivatives may possess agonistic activity with β_2AR. This activity may be much increased in the presence of 3-glucoside as functional group of C3G. In the future, this study may support further investigations on the downstream effects of HGF production induced by C3G in promoting cellular functions, such as cell proliferation and morphogenesis.

In Chapter 4, the author found that HMOs suppressed HUVECs morphology in the presence of TNF-α-induced inflammation. HMOs which is a unique oligosaccharide found in mother's milk also have been shown their potential in modulating growth factor to regulate angiogenesis-like effects, especially for sialyllactose. However, there is still limited study on pooled HMOs effects on the angiogenesis-like morphology induced by TNF-α-stimulated inflammation which is also crucial in intestinal epithelial cells. The author used a model of co-culture Caco-2 and HUVECs to observe the inhibitory effects of HMOs on HUVEC's growth in the presence of TNF-α which stimulates VEGF production from Caco-2. Based on these results, the co-treatment of HMOs and TNF-α showed inhibitory effect on the HUVECs proliferation. Further analysis such as scratch assay and tube formation assay showed the co-treatment of HMOs and TNF-α also demonstrated the suppression effects of angiogenesis-like morphology such as HUVECs migration and tube formation. This study may provide new beneficial effects on HMOs as anti-angiogenesis agents in the development of tumorigenesis. However, further investigations are required to obtain more robust evidence of HMOs effects on VEGF-induced angiogenesis-like morphology, particularly performing quantitative analysis.

Some bioactive compounds, especially extracted from plants is not merely considered as functional food products, but also as essential resources of many medicines and active

pharmaceutical ingredients. In a few clinical studies. C3G have been evidently showed benefits for cardiovascular health, modulating inflammation biomarkers, improving insulin action[85], and anti-cancer activity[86]. C3G may exert significant pharmacological activities towards metabolic effects. Previously, most of bioactive compounds have been extracted only in plants, however, their roles as complementary or alternative medicine have been gradually recognized since they also have been discovered in mammalian products[86]. Currently, food and pharmaceutical industry have been attracted an important family of oligosaccharides composed of HMOs and have strong interest in incorporation of those oligosaccharides into functional or medicinal foods. In addition to nutritional elements, HMOs has been known as bioactive compound in human milk which relate to prevention and treatment of disease such as gastrointestinal, respiratory, immune, and blood system disorders[87]. Current investigations on bioactive compounds towards some clinical trials are still going on, but basic investigations including the mechanisms of their actions, long-term safety, effective dosage, and the unanticipated side effects will have to be thoroughly conducted. Therefore, in this study, the author highlighted the novel mechanisms of actions of food-derived bioactive compounds towards identification of their cellular targets.

The health claims of food-derived components emphasize the associations between dietary nutritional and medical research related to health benefits. The investigations of food-derived components on the prevention potentials of non-communicable diseases, such as heart disease, type II diabetes, cancer, and neurodegenerative diseases have been conducted and documented well. These health outcomes provide scientific evidence to support the application of food-derived components as functional foods which is rapidly growing in the market. Investigations on biological actions driven by food-derived components have become a major concern to support their functionality, the strength of the evidence, and to assure potential applications for a long time.

In this study, food-derived components, including C3G and HMOs was discovered to regulate growth factor production which is the fundamental mechanisms to promote maintenance of tissue homeostasis. Besides, the ability of C3G and HMOs in regulating growth factor production is considered essential to prevent several non-communicable diseases because growth factor is the main regulator for several pathways related to cellular functions. Furthermore, in some cases, the health claims of functional foods do not have sufficiently strong evidence, although they have been known as healthy foods for public health. Therefore, these findings also provide novel and strong scientific evidence to emphasize their health claims as functional foods in the future. The author expected that the discovery of basis information of food-derived components in promoting health outcomes support further advanced investigations for pre-clinical and clinical studies to support the development of functional foods as one of the strategies to optimally enhance health and reduce disease risk.

Acknowledgement

I would like to extend my deepest gratitude to my supervisors, Assoc Prof. Yusaku Miyamae and Prof. Toshikazu Kamiya, for their great support at every stage of my PhD study and also for patiently providing advice, as well as the insightful comments and suggestions during my PhD study. I would like to express my special thanks to my thesis committee reviewers, Prof. Hiroyuki Fuchino, Prof. Sosaku Ichikawa and Assoc Prof. Dong-Zhu Xu for reviewing my thesis with constructive feedbacks. Furthermore, I would like to express my sincere thanks to Prof. Hideyuki Shigemori as a research collaborator and Prof. Hiroko Isoda, as well as Assoc Prof. Shinya Takahashi as my sub-supervisors, for their helpful comment, advice, and suggestion to improve my PhD research and thesis.

In addition, I would like to say my special thanks to my colleagues in Miyamae-sensei's group, Mr. Yuki Utsugi, Mr. Takumi Suzuki, and Ms. Natsu Tokura for their willingness to help my experiments, particularly for teaching me several experimental methods, Ms. Shinano Miyazawa, Ms. Hina Ishii, and Ms. Yang Zhe for their kindness, friendly and cheerful characters for sharing any things, Mr. Damilare Adebowale for his kindness and he is a nice colleague, as well as for Ms. Syarifatul Mufidah, who always supports me in any situations during my PhD study.

I would like to extend my special thanks to T-LSI management for providing good environment for T-LSI students, including me, to keep studying in convenience way and also for my beloved friends in T-LSI, Ms. Anissa Nofita Sari, Ms. Wasiatus Sa'diyah, Ms. Hazna Noor Meidinna, Ms. Ayukireina Prahesti, other friends for their support in my ups and downs. I learnt so many things from them. Furthermore, I would like to express my gratitude to MEXT scholarship as financial support during my study.

I would like to express my deepest gratitude to my beloved husband, Mr. Jupri Reza Dauta. Thank you very much for always be on my side in my ups and downs, for always being a caring and loving husband any time. Your supports really strengthened me out. To my beloved little daughter, Kiyomi Nabila Al Jufri, for always being a good girl and always cheering me up. To my beloved parents and family who always prays goodness for me, especially for my mother who never be tired to support me during PhD study.

Finally, last gratitude words to Allah SWT, the almighty God. All praises and thanks to Allah, the Lord of the Universe.

References

1. Stone, W.; Varacallo, M., Physiology, Growth Factor. **2018**.
2. Cordover, E.; Minden, A., Signaling pathways downstream to receptor tyrosine kinases: targets for cancer treatment. *Journal of Cancer Metastasis and Treatment* **2020,** *6*, 45.
3. Koganti, P.; Levy-Cohen, G.; Blank, M., Smurfs in Protein Homeostasis, Signaling, and Cancer. *Frontiers in Oncology* **2018,** *8*.
4. Ren, X.; Zhao, M.; Lash, B.; Martino, M. M.; Julier, Z., Growth Factor Engineering Strategies for Regenerative Medicine Applications. *Frontiers in bioengineering and biotechnology* **2020,** *7*, 469-469.
5. Williams, M.; Pehu, E.; Ragasa, C., Functional Foods : Opportunities and Challenges for Developing Countries. *Agricultural and Rural Development Note* **2006,** *19*.
6. Krause, J., and Gailene Tobin, *Discovery, development, and regulation of natural products." Using old solutions to new problems-natural drug discovery in the 21st century 1* 2013; p 1-35.
7. Pickens, L. B.; Tang, Y.; Chooi, Y.-H., Metabolic engineering for the production of natural products. *Annu Rev Chem Biomol Eng* **2011,** *2*, 211-236.
8. Dias, D. A.; Urban, S.; Roessner, U., A historical overview of natural products in drug discovery. *Metabolites* **2012,** *2* (2), 303-336.
9. Panche, A. N.; Diwan, A. D.; Chandra, S. R., Flavonoids: an overview. *J Nutr Sci* **2016,** *5*, e47-e47.
10. Havsteen, B. H., The biochemistry and medical significance of the flavonoids. *Pharmacol Ther* **2002,** *96* (2-3), 67-202.
11. Khoo, H. E.; Azlan, A.; Tang, S. T.; Lim, S. M., Anthocyanidins and anthocyanins: colored pigments as food, pharmaceutical ingredients, and the potential health benefits. *Food Nutr Res* **2017,** *61* (1), 1361779.
12. Wahyuningsih, S.; Wulandari, L.; Wartono, M. W.; Munawaroh, H.; Ramelan, A. H. In *The Effect of pH and Color Stability of Anthocyanin on Food Colorant*, Materials Science and Engineering Conference Series, April 01, 2017; 2017; p 012047.
13. Welch, C. R.; Wu, Q.; Simon, J. E., Recent Advances in Anthocyanin Analysis and Characterization. *Curr Anal Chem* **2008,** *4* (2), 75-101.
14. Olivas-Aguirre, F. J.; Rodrigo-García, J.; Martínez-Ruiz, N. D. R.; Cárdenas-Robles, A. I.; Mendoza-Díaz, S. O.; Álvarez-Parrilla, E.; González-Aguilar, G. A.; de la Rosa, L. A.; Ramos-Jiménez, A.; Wall-Medrano, A., Cyanidin-3-O-glucoside: Physical-Chemistry, Foodomics and Health Effects. *Molecules* **2016,** *21* (9), 1264.
15. Choi, K.; Choi, S.-I.; Park, M.; Han, J.-S., Cyanidin-3-O-glucoside Ameliorates Postprandial Hyperglycemia in Diabetic Mice. *Journal of Life Science* **2017,** *27*, 32-37.
16. Boquien, C.-Y., Human Milk: An Ideal Food for Nutrition of Preterm Newborn. *Front Pediatr* **2018,** *6*, 295-295.
17. Soyyilmaz, B.; Miks, M.; Röhrig, C.; Matwiejuk, M.; Meszaros, A.; Vigsnæs, L., The Mean of Milk: A Review of Human Milk Oligosaccharide Concentrations throughout Lactation. *Nutrients* **2021,** *13*, 2737.
18. Vandenplas, Y.; Berger, B.; Carnielli, V. P.; Ksiazyk, J.; Lagström, H.; Sanchez Luna, M.; Migacheva, N.; Mosselmans, J. M.; Picaud, J. C.; Possner, M.; Singhal, A.; Wabitsch, M., Human Milk Oligosaccharides: 2'-Fucosyllactose (2'-FL) and Lacto-N-Neotetraose (LNnT) in Infant Formula. *Nutrients* **2018,** *10* (9).

19. Xu, Y.; Lou, Z.; Lee, S. H., Arctigenin represses TGF-β-induced epithelial mesenchymal transition in human lung cancer cells. *Biochem Biophys Res Commun* **2017,** *493* (2), 934-939.
20. Sutariya, B.; Saraf, M., Betanin, isolated from fruits of Opuntia elatior Mill attenuates renal fibrosis in diabetic rats through regulating oxidative stress and TGF-β pathway. *J Ethnopharmacol* **2017,** *198*, 432-443.
21. Xing, S.; Yu, W.; Zhang, X.; Luo, Y.; Lei, Z.; Huang, D.; Lin, J.; Huang, Y.; Huang, S.; Nong, F.; Zhou, C.; Wei, G., Isoviolanthin Extracted from Dendrobium officinale Reverses TGF-β1-Mediated Epithelial–Mesenchymal Transition in Hepatocellular Carcinoma Cells via Deactivating the TGF-β/Smad and PI3K/Akt/mTOR Signaling Pathways. *Int J Mol Sci* **2018,** *19* (6).
22. Lee, D.; Lim, J.; Woo, K. C.; Kim, K. T., Piperonylic acid stimulates keratinocyte growth and survival by activating epidermal growth factor receptor (EGFR). *Sci Rep* **2018,** *8* (1), 162.
23. Li, X.; Huang, R.; Li, M.; Zhu, Z.; Chen, Z.; Cui, L.; Luo, H.; Luo, L., Parthenolide inhibits the growth of non-small cell lung cancer by targeting epidermal growth factor receptor. *Cancer Cell International* **2020,** *20* (1), 561.
24. Im, H. J.; Li, X.; Chen, D.; Yan, D.; Kim, J.; Ellman, M. B.; Stein, G. S.; Cole, B.; Kc, R.; Cs-Szabo, G.; van Wijnen, A. J., Biological effects of the plant-derived polyphenol resveratrol in human articular cartilage and chondrosarcoma cells. *J Cell Physiol* **2012,** *227* (10), 3488-97.
25. Liu, Q.; Yu, S.; Zhao, W.; Qin, S.; Chu, Q.; Wu, K., EGFR-TKIs resistance via EGFR-independent signaling pathways. *Molecular Cancer* **2018,** *17* (1), 53.
26. Guo, D.; Murdoch, C. E.; Liu, T.; Qu, J.; Jiao, S.; Wang, Y.; Wang, W.; Chen, X., Therapeutic Angiogenesis of Chinese Herbal Medicines in Ischemic Heart Disease: A Review. *Frontiers in Pharmacology* **2018,** *9*.
27. Rezzola, S.; Loda, A.; Corsini, M.; Semeraro, F.; Annese, T.; Presta, M.; Ribatti, D., Angiogenesis-Inflammation Cross Talk in Diabetic Retinopathy: Novel Insights From the Chick Embryo Chorioallantoic Membrane/Human Vitreous Platform. *Frontiers in Immunology* **2020,** *11*.
28. Nakamura, T.; Mizuno, S., The discovery of hepatocyte growth factor (HGF) and its significance for cell biology, life sciences and clinical medicine. *Proc Jpn Acad Ser B Phys Biol Sci* **2010,** *86* (6), 588-610.
29. Nakamura, T.; Sakai, K.; Nakamura, T.; Matsumoto, K., Hepatocyte growth factor twenty years on: Much more than a growth factor. *J Gastroenterol Hepatol* **2011,** *26 Suppl 1*, 188-202.
30. Stoker, M.; Gherardi, E.; Perryman, M.; Gray, J., Scatter factor is a fibroblast-derived modulator of epithelial cell mobility. *Nature* **1987,** *327* (6119), 239-242.
31. Kato, E.; Kimura, S.; Kawabata, J., Ability of higenamine and related compounds to enhance glucose uptake in L6 cells. *Bioorg Med Chem* **2017,** *25* (24), 6412-6416.
32. Matsumoto, K.; Funakoshi, H.; Takahashi, H.; Sakai, K., HGF-Met Pathway in Regeneration and Drug Discovery. *Biomedicines* **2014,** *2* (4), 275-300.
33. Ono, T.; Tsuji, T.; Sakai, M.; Yukizaki, C.; Ino, H.; Akagi, I.; Hiramatsu, K.; Matsumoto, Y.; Sugiura, Y.; Uto, H.; Tsubouchi, H.; Gohda, E., Induction of hepatocyte growth factor production in human dermal fibroblasts and their proliferation by the extract of bitter melon pulp. *Cytokine* **2009,** *46* (1), 119-26.
34. Kurisu, M.; Nakasone, R.; Miyamae, Y.; Matsuura, D.; Kanatani, H.; Yano, S.; Shigemori, H., Induction of hepatocyte growth factor production in human dermal fibroblasts by caffeic acid derivatives. *Biol Pharm Bull* **2013,** *36* (12), 2018-21.

35. Nakasone, R.; Kurisu, M.; Onodera, M.; Miyamae, Y.; Matsuura, D.; Kanatani, H.; Yano, S., Promoting Effects on Hepatocyte Growth Factor Production of Daphnane Diterpenoids from Daphne odora. *HETEROCYCLES* **2013,** *87*, 1087.
36. Simons, M.; Gordon, E.; Claesson-Welsh, L., Mechanisms and regulation of endothelial VEGF receptor signalling. *Nat Rev Mol Cell Biol* **2016,** *17* (10), 611-25.
37. Chung, T. W.; Kim, S. J.; Choi, H. J.; Kwak, C. H.; Song, K. H.; Suh, S. J.; Kim, K. J.; Ha, K. T.; Park, Y. G.; Chang, Y. C.; Chang, H. W.; Lee, Y. C.; Kim, C. H., CAPE suppresses VEGFR-2 activation, and tumor neovascularization and growth. *J Mol Med (Berl)* **2013,** *91* (2), 271-82.
38. Aguilar-Cazares, D., Contribution of angiogenesis to inflammation and cancer. *Frontiers in oncology* **2019**, 1399.
39. Munn, L. L., Cancer and inflammation. *WIREs Systems Biology and Medicine* **2017,** *9* (2), e1370.
40. Weimar, I. S.; Voermans, C.; Bourhis, J. H.; Miranda, N.; van den Berk, P. C.; Nakamura, T.; de Gast, G. C.; Gerritsen, W. R., Hepatocyte growth factor/scatter factor (HGF/SF) affects proliferation and migration of myeloid leukemic cells. *Leukemia* **1998,** *12* (8), 1195-203.
41. Ishigaki, A.; Aoki, M.; Nagai, M.; Warita, H.; Kato, S.; Kato, M.; Nakamura, T.; Funakoshi, H.; Itoyama, Y., Intrathecal delivery of hepatocyte growth factor from amyotrophic lateral sclerosis onset suppresses disease progression in rat amyotrophic lateral sclerosis model. *J Neuropathol Exp Neurol* **2007,** *66* (11), 1037-44.
42. Morishita, R.; Nakamura, S.; Hayashi, S.; Taniyama, Y.; Moriguchi, A.; Nagano, T.; Taiji, M.; Noguchi, H.; Takeshita, S.; Matsumoto, K.; Nakamura, T.; Higaki, J.; Ogihara, T., Therapeutic angiogenesis induced by human recombinant hepatocyte growth factor in rabbit hind limb ischemia model as cytokine supplement therapy. *Hypertension* **1999,** *33* (6), 1379-84.
43. Nagoshi, N.; Tsuji, O.; Kitamura, K.; Suda, K.; Maeda, T.; Yato, Y.; Abe, T.; Hayata, D.; Matsumoto, M.; Okano, H.; Nakamura, M., Phase I/II Study of Intrathecal Administration of Recombinant Human Hepatocyte Growth Factor in Patients with Acute Spinal Cord Injury: A Double-Blind, Randomized Clinical Trial of Safety and Efficacy. *J Neurotrauma* **2020,** *37* (15), 1752-1758.
44. Matsukawa, T.; Motojima, H.; Sato, Y.; Takahashi, S.; Villareal, M.; Isoda, H., Upregulation of skeletal muscle PGC-1α through the elevation of cyclic AMP levels by Cyanidin-3-glucoside enhances exercise performance. *Scientific Reports* **2017,** *7*, 44799.
45. Matsukawa, T.; Inaguma, T.; Han, J.; Villareal, M. O.; Isoda, H., Cyanidin-3-glucoside derived from black soybeans ameliorate type 2 diabetes through the induction of differentiation of preadipocytes into smaller and insulin-sensitive adipocytes. *J Nutr Biochem* **2015,** *26* (8), 860-7.
46. Gohda, E.; Kataoka, H.; Tsubouchi, H.; Daikilara, Y.; Yamamoto, I., Phorbol ester-induced secretion of human hepatocyte growth factor by human skin fibroblasts and its inhibition by dexamethasone. *FEBS Letters* **1992,** *301* (1), 107-110.
47. Li, W.; Fan, J.; Chen, M.; Guan, S.; Sawcer, D.; Bokoch, G. M.; Woodley, D. T., Mechanism of human dermal fibroblast migration driven by type I collagen and platelet-derived growth factor-BB. *Mol Biol Cell* **2004,** *15* (1), 294-309.
48. Delghandi, M. P.; Johannessen, M.; Moens, U., The cAMP signalling pathway activates CREB through PKA, p38 and MSK1 in NIH 3T3 cells. *Cell Signal* **2005,** *17* (11), 1343-51.
49. Seamon, K. B.; Padgett, W.; Daly, J. W., Forskolin: unique diterpene activator of adenylate cyclase in membranes and in intact cells. *Proc Natl Acad Sci U S A* **1981,** *78* (6), 3363-7.

50. Nasu, K.; Sugano, T.; Matsui, N.; Narahara, H.; Kawano, Y.; Miyakawa, I., Expression of Hepatocyte Growth Factor in Cultured Human Endometrial Stromal Cells Is Induced through a Protein Kinase C-Dependent Pathway. *Biology of Reproduction* **1999,** *60* (5), 1183-1187.
51. Chattopadhyay, N.; Tfelt-Hansen, J.; Brown, E. M., PKC, p42/44 MAPK and p38 MAPK regulate hepatocyte growth factor secretion from human astrocytoma cells. *Brain Res Mol Brain Res* **2002,** *102* (1-2), 73-82.
52. Murray, A. J., Pharmacological PKA inhibition: all may not be what it seems. *Sci Signal* **2008,** *1* (22), re4.
53. Liu, C.; Ke, P.; Zhang, J.; Zhang, X.; Chen, X., Protein Kinase Inhibitor Peptide as a Tool to Specifically Inhibit Protein Kinase A. *Front Physiol* **2020,** *11*, 574030.
54. Matsunaga, T.; Gohda, E.; Takebe, T.; Wu, Y. L.; Iwao, M.; Kataoka, H.; Yamamoto, I., Expression of hepatocyte growth factor is up-regulated through activation of a cAMP-mediated pathway. *Exp Cell Res* **1994,** *210* (2), 326-35.
55. Sassone-Corsi, P., The cyclic AMP pathway. *Cold Spring Harb Perspect Biol* **2012,** *4* (12).
56. Naqvi, S.; Martin, K. J.; Arthur, J. S., CREB phosphorylation at Ser133 regulates transcription via distinct mechanisms downstream of cAMP and MAPK signalling. *Biochem J* **2014,** *458* (3), 469-79.
57. Mayr, B. M.; Canettieri, G.; Montminy, M. R., Distinct effects of cAMP and mitogenic signals on CREB-binding protein recruitment impart specificity to target gene activation via CREB. *Proceedings of the National Academy of Sciences of the United States of America* **2001,** *98* (19), 10936-10941.
58. Hudson, C.; Kimura, T. E.; Duggirala, A.; Sala-Newby, G. B.; Newby, A. C.; Bond, M., Dual Role of CREB in The Regulation of VSMC Proliferation: Mode of Activation Determines Pro- or Anti-Mitogenic Function. *Scientific Reports* **2018,** *8* (1), 4904.
59. Li, G.; Peng, X.; Guo, Y.; Gong, S.; Cao, S.; Qiu, F., Currently Available Strategies for Target Identification of Bioactive Natural Products. *Front Chem* **2021,** *9*, 761609.
60. Wang, H.; Wang, C.; Zou, Y.; Hu, J.; Li, Y.; Cheng, Y., Natural polyphenols in drug delivery systems: Current status and future challenges. *Giant* **2020,** *3*, 100022.
61. Chen, X.; Wang, Y.; Ma, N.; Tian, J.; Shao, Y.; Zhu, B.; Wong, Y. K.; Liang, Z.; Zou, C.; Wang, J., Target identification of natural medicine with chemical proteomics approach: probe synthesis, target fishing and protein identification. *Signal Transduction and Targeted Therapy* **2020,** *5* (1), 72.
62. Jia, Y.; Wu, C.; Kim, Y.-S.; Yang, S. O.; Kim, Y.; Kim, J.-S.; Jeong, M.-Y.; Lee, J. H.; Kim, B.; Lee, S.; Oh, H.-S.; Kim, J.; So, M.-Y.; Yoon, Y. E.; Thach, T. T.; Park, T. H.; Lee, S.-J., A dietary anthocyanin cyanidin-3-O-glucoside binds to PPARs to regulate glucose metabolism and insulin sensitivity in mice. *Communications Biology* **2020,** *3* (1), 514.
63. Menzaghi, F.; Behan, D. P.; Chalmers, D. T., Constitutively activated G protein-coupled receptors: a novel approach to CNS drug discovery. *Curr Drug Targets CNS Neurol Disord* **2002,** *1* (1), 105-21.
64. Wu, Y.; Zeng, L.; Zhao, S., Ligands of Adrenergic Receptors: A Structural Point of View. *Biomolecules* **2021,** *11* (7).
65. Bai, C.; Wang, J.; Mondal, D.; Du, Y.; Ye, R. D.; Warshel, A., Exploring the Activation Process of the β2AR-Gs Complex. *Journal of the American Chemical Society* **2021,** *143* (29), 11044-11051.

66. Zheng, M.; Zhu, W.; Han, Q.; Xiao, R.-P., Emerging concepts and therapeutic implications of β-adrenergic receptor subtype signaling. *Pharmacology & Therapeutics* **2005,** *108* (3), 257-268.
67. Tripathi, A.; Kumar, M.; Kaur, P.; Kumar, B.; Sagi, S. S. K., Efficacy of Quercetin as a potent sensitizer of β2-AR in combating the impairment of fluid clearance in lungs of rats under hypoxia. *Respir Physiol Neurobiol* **2020,** *273*, 103334.
68. Motohashi, K., A simple and efficient seamless DNA cloning method using SLiCE from Escherichia coli laboratory strains and its application to SLiP site-directed mutagenesis. *BMC Biotechnology* **2015,** *15* (1), 47.
69. Mutlu, G. M.; Factor, P., Alveolar epithelial beta2-adrenergic receptors. *Am J Respir Cell Mol Biol* **2008,** *38* (2), 127-34.
70. Jean-Charles, P.-Y.; Kaur, S.; Shenoy, S. K., G Protein-Coupled Receptor Signaling Through β-Arrestin-Dependent Mechanisms. *J Cardiovasc Pharmacol* **2017,** *70* (3), 142-158.
71. Lacroix, S.; Klicic Badoux, J.; Scott-Boyer, M.-P.; Parolo, S.; Matone, A.; Priami, C.; Morine, M. J.; Kaput, J.; Moco, S., A computationally driven analysis of the polyphenol-protein interactome. *Scientific Reports* **2018,** *8* (1), 2232.
72. Ring, A. M.; Manglik, A.; Kruse, A. C.; Enos, M. D.; Weis, W. I.; Garcia, K. C.; Kobilka, B. K., Adrenaline-activated structure of β2-adrenoceptor stabilized by an engineered nanobody. *Nature* **2013,** *502* (7472), 575-579.
73. Penn, R. B.; Bond, R. A.; Walker, J. K. L., GPCRs and arrestins in airways: implications for asthma. *Handb Exp Pharmacol* **2014,** *219*, 387-403.
74. Masureel, M.; Zou, Y.; Picard, L.-P.; van der Westhuizen, E.; Mahoney, J. P.; Rodrigues, J. P. G. L. M.; Mildorf, T. J.; Dror, R. O.; Shaw, D. E.; Bouvier, M.; Pardon, E.; Steyaert, J.; Sunahara, R. K.; Weis, W. I.; Zhang, C.; Kobilka, B. K., Structural insights into binding specificity, efficacy and bias of a β2AR partial agonist. *Nature Chemical Biology* **2018,** *14* (11), 1059-1066.
75. Whalen, E. J.; Rajagopal, S.; Lefkowitz, R. J., Therapeutic potential of β-arrestin- and G protein-biased agonists. *Trends Mol Med* **2011,** *17* (3), 126-39.
76. Balbaa, M., Importance of Growth Factors. *Biochemistry & Physiology: Open Access* **2013,** *02*.
77. Wesche, J.; Haglund, K.; Haugsten, E. M., Fibroblast growth factors and their receptors in cancer. *Biochem J* **2011,** *437* (2), 199-213.
78. Rajabi, M.; Mousa, S. A., The Role of Angiogenesis in Cancer Treatment. *Biomedicines* **2017,** *5* (2).
79. Nishida, N.; Yano, H.; Nishida, T.; Kamura, T.; Kojiro, M., Angiogenesis in cancer. *Vasc Health Risk Manag* **2006,** *2* (3), 213-9.
80. Toaldo, I. M.; Van Camp, J.; Gonzales, G. B.; Kamiloglu, S.; Bordignon-Luiz, M. T.; Smagghe, G.; Raes, K.; Capanoglu, E.; Grootaert, C., Resveratrol improves TNF-α-induced endothelial dysfunction in a coculture model of a Caco-2 with an endothelial cell line. *J Nutr Biochem* **2016,** *36*, 21-30.
81. Poliseno, L.; Tuccoli, A.; Mariani, L.; Evangelista, M.; Citti, L.; Woods, K.; Mercatanti, A.; Hammond, S.; Rainaldi, G., MicroRNAs modulate the angiogenic properties of HUVECs. *Blood* **2006,** *108* (9), 3068-71.
82. Ruder, B.; Atreya, R.; Becker, C., Tumour Necrosis Factor Alpha in Intestinal Homeostasis and Gut Related Diseases. *Int J Mol Sci* **2019,** *20* (8).

83. Guo, S.; Lok, J.; Liu, Y.; Hayakawa, K.; Leung, W.; Xing, C.; Ji, X.; Lo, E. H., Assays to examine endothelial cell migration, tube formation, and gene expression profiles. *Methods Mol Biol* **2014,** *1135*, 393-402.
84. Goodwin, A. M., In vitro assays of angiogenesis for assessment of angiogenic and anti-angiogenic agents. *Microvasc Res* **2007,** *74* (2-3), 172-83.
85. Ferrari, D.; Cimino, F.; Fratantonio, D.; Molonia, M. S.; Bashllari, R.; Busà, R.; Saija, A.; Speciale, A., Cyanidin-3-O-Glucoside Modulates the In Vitro Inflammatory Crosstalk between Intestinal Epithelial and Endothelial Cells. *Mediators of Inflammation* **2017,** *2017*, 3454023.
86. Cho, E.; Chung, E. Y.; Jang, H. Y.; Hong, O. Y.; Chae, H. S.; Jeong, Y. J.; Kim, S. Y.; Kim, B. S.; Yoo, D. J.; Kim, J. S.; Park, K. H., Anti-cancer Effect of Cyanidin-3-glucoside from Mulberry via Caspase-3 Cleavage and DNA Fragmentation in vitro and in vivo. *Anticancer Agents Med Chem* **2017,** *17* (11), 1519-1525.
87. Pérez-Escalante, E.; Alatorre-Santamaría, S.; Castañeda-Ovando, A.; Salazar-Pereda, V.; Bautista-Ávila, M.; Cruz-Guerrero, A. E.; Flores-Aguilar, J. F.; González-Olivares, L. G., Human milk oligosaccharides as bioactive compounds in infant formula: recent advances and trends in synthetic methods. *Crit Rev Food Sci Nutr* **2022,** *62* (1), 181-214.